


TR-FOU-2328-5			 aquastuctures
			Page 1 of 42
Author: HNM	Verified: AJB	Revision: 9	Published: 08.10.2024




---

# Loads on General impermeable nets and large volume objects in AquaSim

TR-FOU-2328-5

Revision: 9

---

TR-FOU-2328-5			 Page 2 of 42
Author: HNM	Verified: AJB	Revision: 9	Published: 08.10.2024

Report no.:	TR-FOU-2328-5		
Date of this revision:	08.10.2024		
Number of pages:	42		
Distribution:	Open		
Author:	Are Johan Berstad	Keywords:	Finite Element Analysis Hydrodynamic hydrostatic General impermeable net

**Summary:**

This document describes how hydrostatic- and hydrodynamic forces are calculated in AquaSim for the load formulation General impermeable nets, including Lice skirt, Closed compartment, and Surface tarpaulin.

Verifications of the numerical calculation of diffraction forces by comparing MacCamy Fuchs and numerical solution to analytical solutions for cases where the water is acting on a stiff object. Further, the report outlines a load model for a fully flexible tarp and shows how to combine this load model with the diffraction load model to obtain a hybrid load model applicable for tubes or lice skirts.

**Revision 7:**

As from AquaSim version 2.19.1, the load formulation for calculating drag and lift forces to membrane panels have been modified. Theory for the revised formulation is given in section 2.2.1.

Case studies in section 3.3 updated according to changes in solver 2.19.1. This includes comparison of tank test and AquaSim analysis of a tube.


**Revision 8:**

Corrections Table 1.

**Revision 9:**


Corrections section 2.4.

9	08.10.2024	HNM	AJB	Corrections section 2.4
8	27.09.2024	HNM	AJB	Corrections
7	17.06.2024	AJB & HNM	ISH	Drag and lift force calculations revised
6	26.01.2024	AJB	ISH	Pressure coefficient revised
5	19.01.2021	AJB	LFH	-
4	06.08.2020	AJB	LFH	-
3	29.05.2020	AJB	LFH	-
2	19.05.2020	AJB	LFH	-
1	09.12.2019	AJB	ISH	-
Revision no.	Date	Author	Verified by	Description

TR-FOU-2328-5			 Page 3 of 42
Author: HNM	Verified: AJB	Revision: 9	Published: 08.10.2024

# Content

1	Introduction.....	4
2	Sea loads to objects in water.....	4
2.1	Hydrostatic forces.....	4
2.1.1	Buoyancy forces.....	5
2.2	Current- and viscous forces.....	6
2.2.1	Forces from current flow around an impermeable structure.....	6
2.3	Waves.....	13
2.3.1	Hydrodynamic forces to a stiff body.....	15
2.4	Hydrodynamic force to a flexible tarpaulin.....	17
2.5	Added mass and damping.....	18
2.5.1	Hydrodynamic added mass and damping.....	18
2.5.2	Notes on damping.....	19
2.6	Wave drift forces.....	19
2.7	Hybrid load model.....	20
2.8	In and out of the waterline.....	20
2.9	Waves and current combined.....	20
3	Case studies.....	21
3.1	Vertical stiff cylinder.....	21
3.2	Case compared to reflection from wall.....	24
3.3	Flexible tube net.....	26
3.3.1	Testing and comparison current.....	28
3.3.2	Testing and comparison regular waves with current.....	34
3.3.3	Results discussion.....	39
4	Conclusion.....	40
5	References.....	41

TR-FOU-2328-5			 aquastructures Page 4 of 42
Author: HNM	Verified: AJB	Revision: 9	Published: 08.10.2024

# 1 Introduction

This report shows how hydrostatic and hydrodynamic forces are calculated in AquaSim for the load formulation General impermeable net. As Lice skirt, Closed compartment and Surface tarpaulin is all based on General impermeable net, this report is also valid for these load formulations.

In AquaSim the diffraction forces on an object can be estimated either by MacCamy Fuchs theory or by a numerical estimate, and the user can scale these load components to obtain an approximation for flexible tarp. (A tarp or tarpaulin, is a large sheet of strong, flexible, water-resistant, or waterproof material, often cloth such as canvas or polyester coated with polyurethane or made of plastics such as polyethylene.)

This report verifies the numerical calculation of diffraction forces by comparing MacCamy Fuchs and numerical solutions to analytical solutions for cases where the water is acting on a stiff object. The report outlines a load model for a fully flexible tarp and shows how to combine this load model with the diffraction load model to obtain a hybrid load model applicable for tubes or lice skirts. This model is compared to model test results for a tube. The results are discussed in light of the load model.

## 2 Sea loads to objects in water

As an introduction, an overview of forces to objects in water is given firstly.

### 2.1 Hydrostatic forces

Consider an object floating in water, as shown in Figure 1. It is partly submerged with a width  $b$  and draught  $h$ . The length  $l$  is along the x-axis.

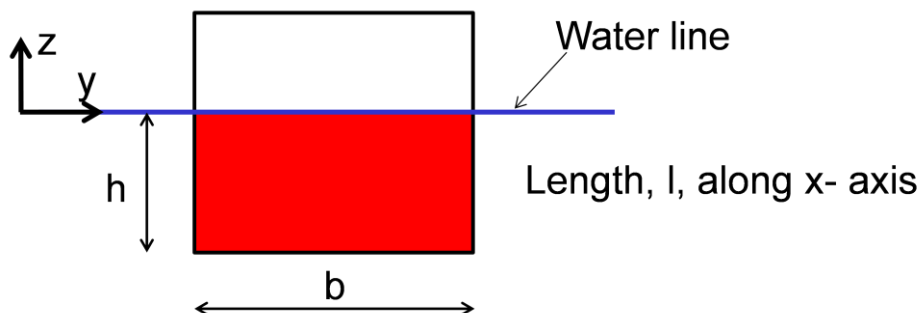


Figure 1 Rectangular object seen in the yz-plane

## 2.1.1 Buoyancy forces

The forces acting from the water to the structure is the integral of the fluid pressure around the object. Define an orthonormal coordinate system where the x- axis is along the object in the horizontal plane, the z- axis is upwards with origin at the mean water line. Hydrostatic pressure increases downwards in a fluid, and the hydrostatic pressure at a given point in a fluid can be found as (see e.g. (Hydrostatics, 2024)):

$$p = -\rho g z + p_{atm}$$

*Equation 1*

where  $\rho$  is the fluid density,  $g$  is gravity,  $z$  is the vertical location (origin at free surface and axis pointing upwards), and  $p_{atm}$  us the atmospheric pressure in air at the free surface.

Assume the fluid is non-viscous. Then a force originating by fluid pressure will be directed normal to the surface. Introducing this to the case seen in Figure 1 it is seen that the net horizontal force is 0 due to symmetry, and the net vertical force is:

$$F = \rho g h b l$$

*Equation 2*

where  $F$  is positive upwards, and  $l$  is the length out of the plane, seen in Figure 1, and  $h$  and  $b$  are defined in the same figure. Equation 1 can be rewritten:

$$F = \rho g V$$

*Equation 3*

where  $V$  is the submerged volume. As seen, this is in accordance with Archimedes principle (see e.g. (Archimede's principle, 2024)).

Consider a case where there is just a net without closed bottom as seen in Figure 2. In this case the static pressure from water will be equal on the inside and the outside.

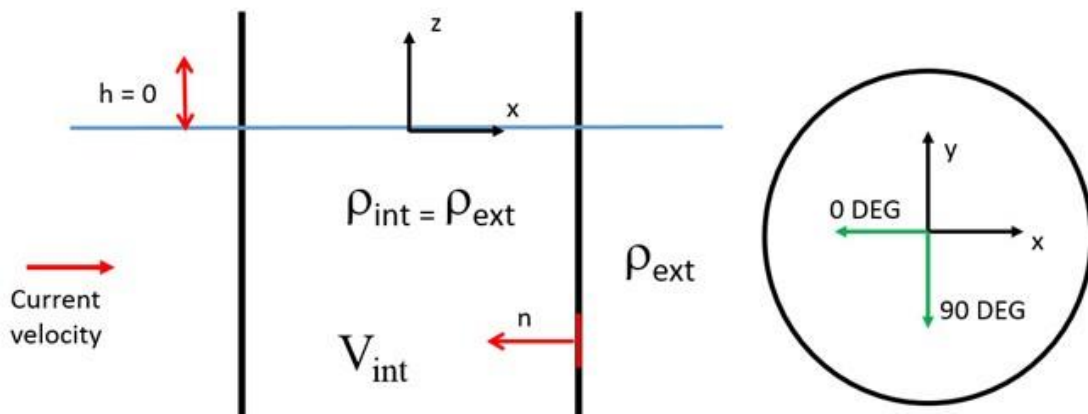


*Figure 2 Impermeable net exposed to current flow*

## 2.2 Current- and viscous forces

For regular fish farms based on twine (threads) nets, the forces caused by current are normally the largest environmental load. The physics of impermeable nets are different, and the flow cannot pass through the object. This section exemplifies this with a cylinder which is a very relevant shape for aquaculture units. drag force acting on the cylinder.

The formulation of how pressure from current originally (earlier than version 2.19.0) was handled in AquaSim is given in (Aquastructures, 2019).

### 2.2.1 Forces from current flow around an impermeable structure

Drag force to an object is the force in line with the incident fluid flow and lift is the force perpendicular to the flow, this is illustrated in Figure 3.

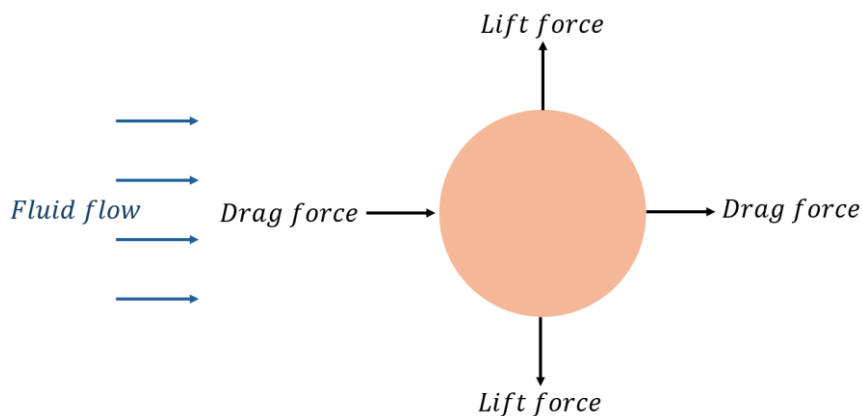


Figure 3 Drag- and lift forces with respect to direction of fluid flow

Figure 4 shows flow around a cylinder for a laboratory test. The velocity field will introduce a pressure field around the cylinder.

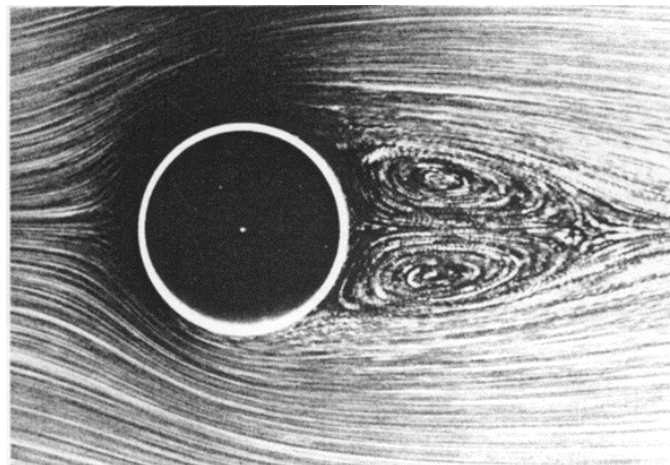


Figure 4 Streamlines of flow passing a cylinder (Barkley, 2006)

It is the pressure-field on the cylinder, integrated around the circumference, which leads to the drag force acting on the cylinder.

Figure 5 show a typical distribution of this pressure to a 2D surface caused by fluid flow around a cylinder. The pressure is converted to a coefficient  $C_p$  (vertical axis in Figure 5). The position around the cylinder in terms of degrees is given in the horizontal axis, which is denoted  $\theta$ .  $0 < \theta < 90$  correspond to the upstream portion of the circle, and  $90 < \theta < 180$  is downstream on the leeward side. Positive values for  $C_p$  mean that pressure is exerted onto the cylinder, while negative values mean a vacuum is acting on the surface.

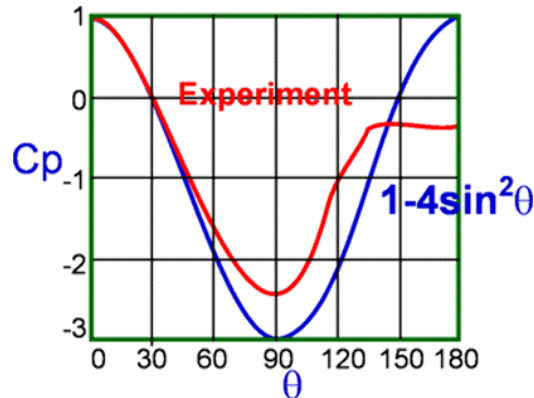


Figure 5 Pressure-field to cylinder surface by flow around it (Flow around a cylinder, 2024)

Figure 6 show how the pressure field vary with Reynolds numbers, and hence have different drag coefficients.

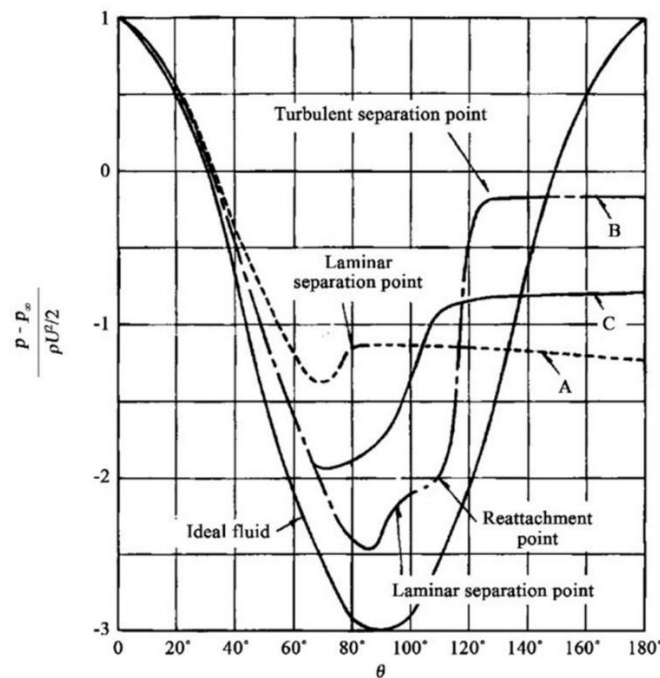


Figure 6 Pressure distribution as function of Reynolds number (Ogawa S., 2018)

In AquaSim, the distribution of the pressure is done in terms of the drag coefficient  $C_D$ , the skin friction coefficient  $C_t$  and a lift coefficient  $C_l$ . The drag and lift coefficients should be interpreted as local drag and lift coefficients for the membrane panel under consideration, which will be elaborate further in the sections below.

To account for varying pressure around the structure, AquaSim enables adjustment of the drag coefficient, locally, based on whether the membrane panel under consideration is located upstream or downstream relative to the flow. The succeeding text and figures show how the coefficients given as input to AquaSim is transferred to local lift, skin friction and drag forces acting on each membrane panel and how it relates to the global drag and lift forces acting on the entire structure.

Consider a case where a cylinder is modelled with several membrane panels as shown in Figure 7. On each panel, a unit normal vector, denoted  $N$ , is pointing outwards, as shown by the blue axis on the highlighted panel in Figure 7. AquaSim calculates pressure on each membrane panel, by using the cross-flow principle in a modified manner.

Locally, the relative velocity between the membrane panel and the fluid flow,  $U_{rel}$ , is decomposed into a normal- and tangential component, where the normal direction is defined by the unit normal vector  $N$ , which is based on the modelled geometry, as described above. Furthermore, the unit tangential vector, denoted  $t$ , is found as:

$$t = \frac{U_{rel} - (N \cdot U_{rel})N}{|U_{rel} - (N \cdot U_{rel})N|}$$

Equation 4

where

- $N$  is the unit normal vector
- $U_{rel}$  is a vector describing the relative velocity between the membrane panel and the fluid flow.

The appropriate local drag- and lift force is then calculated as described by Equation 5 and Equation 8, using the normal- and tangential component of the relative fluid velocity, as well as the total relative velocity.

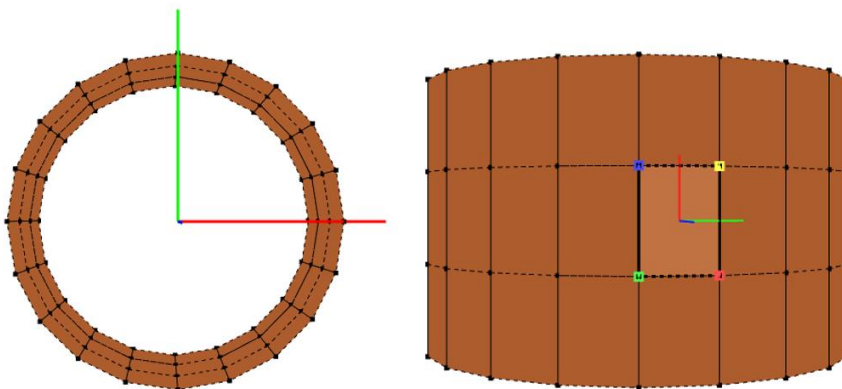



Figure 7 Left: cylinder seen from above. Right: membrane panel with normal (blue line) pointing outwards



TR-FOU-2328-5			 Page 9 of 42
Author: HNM	Verified: AJB	Revision: 9	Published: 08.10.2024

Using a modified version of the cross-flow principle, the local drag force on the panel is calculated as:

$$F_{D_{Local}} = \frac{\rho_w C_d A}{2} (u_N - v_N) |U_{rel}|$$

Equation 5

where

- $\rho_w$  is fluid density,
- $C_d$  is the drag coefficient (AquaEdit input),
- $A$  is area of the membrane panel,
- $u_N$  is the velocity of the incident fluid flow normal to the panel,
- $v_N$  is the velocity of the panel in normal direction,
- $U_{rel}$  is a vector describing the relative velocity between the membrane panel and the fluid flow.

Initially the local lift force on the panel is calculated as:

$$F_{L_{Local_0}} = \frac{\rho_w C_l A}{2} (u_t - v_t) |u_t - v_t|$$

Equation 6

where

- $\rho_w$  is fluid density,
- $C_l$  is the lift coefficient (AquaEdit input),
- $u_t$  is the velocity of the incident fluid flow tangential to the panel,
- $v_t$  is the velocity of the panel in tangential direction,
- $A$  is area of the membrane panel,

Then the vertical component of the lift force is set to 0, meaning that, given the following,

$$F_{L_{Local_0}} N = [F_{L_{Local_x}}, F_{L_{Local_y}}, F_{L_{Local_z}}]$$

Equation 7

where


- $F_{L_{Local_x}}$  is the component of the local lift force on the panel in the global x-direction,
- $F_{L_{Local_y}}$  is the component of the local lift force on the panel in the global y-direction,
- $F_{L_{Local_z}}$  is the component of the local lift force on the panel in the global z-direction,

then the final local lift force on the panel is found as,

$$F_{L_{Local}} = \left| \left[ F_{L_{Local_x}}, F_{L_{Local_y}}, 0 \right] \right| = |F_{L_{Local_x}} \hat{i} + F_{L_{Local_y}} \hat{j}|$$

Equation 8

where

TR-FOU-2328-5			 Page 10 of 42
Author: HNM	Verified: AJB	Revision: 9	Published: 08.10.2024

- $\hat{i}$  is the unit vector pointing in the global x-direction,
- $\hat{j}$  is the unit vector pointing in the global y-direction.

The local lift force is defined to always be pointing outwards from the cylinder, creating suction, as illustrated in Figure 3.

In addition, it is possible in AquaSim to include skin friction drag acting on the panel in the local tangential direction, described by the tangential vector  $t$ . The skin friction drag is calculated as:

$$F_{tLocal} = \frac{\rho_w C_t A}{2} (u_t - v_t) |u_t - v_t|$$

Equation 9

where

- $\rho_w$  is fluid density,
- $C_t$  is the skin friction coefficient for drag in tangential direction (AquaEdit input),
- $u_t$  is the velocity of the incident fluid flow tangential to the panel,
- $v_t$  is the velocity of the panel in tangential direction,
- $A$  is area of the membrane panel.

Furthermore, the contribution from each membrane panel to the global drag and lift forces of the entire structure, can be found by decomposing the local drag, lift and skin friction forces of the membrane panel in the global drag and lift directions. The global drag direction is typically defined to be acting in the same direction as the relative velocity  $U_{rel}$  and could be described by the unit vector  $u$ , which is defined as:

$$u = \frac{U_{rel}}{|U_{rel}|}$$

Equation 10

while the global lift direction typically is defined to be acting perpendicular to the global drag direction, and can be described by the unit vector  $l$ , given by:

$$l = \frac{(N \times u) \times u}{|(N \times u) \times u|}$$

Equation 11

The contribution to the global drag force from a membrane panel can be calculated as,

$$F_{DGlobal} = F_{DLocal} N \cdot u - (F_{LLocal_x} \hat{i} + F_{LLocal_y} \hat{j}) \cdot u + F_{tLocal} t \cdot u$$

Equation 12

while the contribution to the global lift force from a membrane panel can be calculated as,

$$F_{LGlobal} = -F_{DLocal} N \cdot l + (F_{LLocal_x} \hat{i} + F_{LLocal_y} \hat{j}) \cdot l + F_{tLocal} t \cdot l$$

Equation 13

where

- $F_{D_{Local}}$  is the local drag force on the panel,
- $F_{L_{Localx}}$  is the component of the local lift force on the panel in the global x-direction,
- $F_{L_{Localy}}$  is the component of the local lift force on the panel in the global y-direction,
- $F_{t_{Local}}$  is the local skin friction drag force on the panel,
- $N$  is the unit normal vector,
- $u$  is the unit vector pointing in the same direction as the relative velocity  $U_{rel}$ ,
- $t$  is the unit tangential vector,
- $l$  is the unit lift vector pointing in the global lift direction
- $\hat{i}$  is the unit vector pointing in the global x-direction,
- $\hat{j}$  is the unit vector pointing in the global y-direction.

In general, one membrane panel could be part of a larger structure. The “Drag coefficient upstream” given as input in AquaEdit represent the local drag coefficient that is applied in the calculations of the pressure upstream ( $C_{d\ UPSTREAM}$ ) on the structure as shown in Figure 8, while there is an additional input “Drag coefficient downstream” that is used in the calculations of the downstream pressure ( $C_{d\ DOWNSTREAM}$ ).

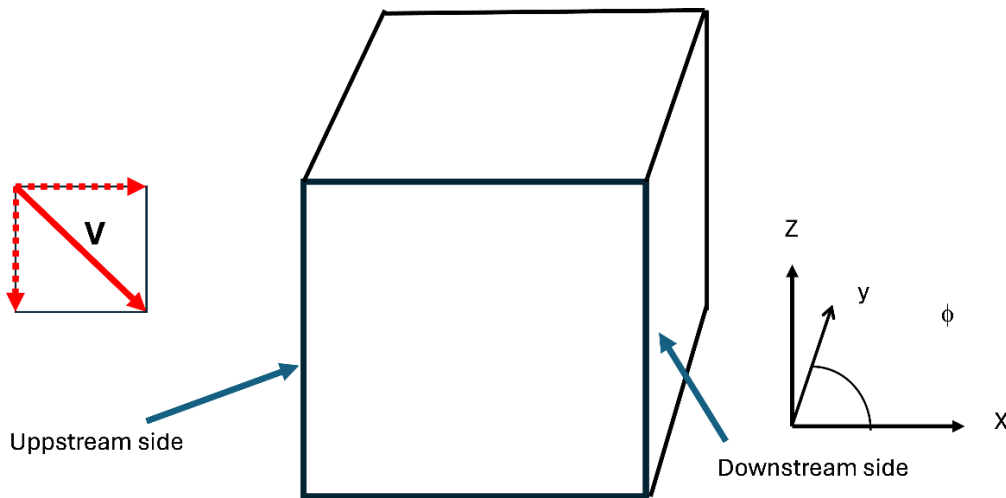


Figure 8 Current into a generic impermeable structure

As an example, by assuming a circular cylinder as shown in Figure 9 and the pressure distribution from the blue curve in Figure 5, the global drag coefficient of the structure is obtained by distributing the local upstream and downstream drag coefficients as described in Table 1. In Table 1,  $C_d$  denotes the global drag coefficient that is achieved,  $C_{d\ UPSTREAM}$  is the local drag coefficient applied on cylinder panels located 0-90 degrees with respect to the fluid flow and  $C_{d\ DOWNSTREAM}$  is the local drag coefficient applied from 90-180 degrees.

Table 1 Example of distribution of drag coefficient around a circular cylinder in AquaSim in order to target a global drag coefficient  $C_d$

Cd upstream	Cd downstream	Corresponding global Cd*
0.00	0.00	0.00
0.75	0.00	0.50
1.00	0.00	0.67
1.00	0.50	1.00
1.00	0.80	1.20
1.00	1.00	1.33
1.00	1.25	1.50
1.00	2.00	2.00
1.25	2.50	2.50
1.50	3.00	3.00

\* Corresponding global  $C_d$ , when integrating  $C_{d\ UPSTREAM}$  and  $C_{d\ DOWNSTREAM}$  around a circle based on pressure distribution from the blue curve in Figure 5.

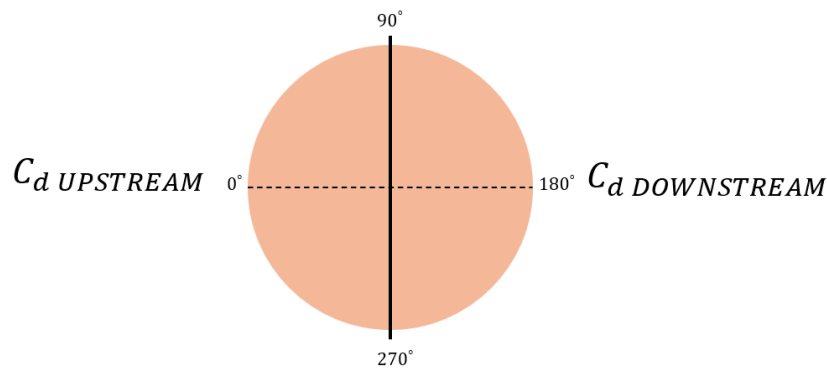


Figure 9 Example of distribution of the local drag coefficient upstream ( $C_{d\ UPSTREAM}$ ) and downstream ( $C_{d\ DOWNSTREAM}$ ) around a circular cylinder in order to target a global drag coefficient  $C_d$

The default values in AquaEdit for the “Drag coefficient upstream”, “Drag coefficient downstream”, “Lift coefficient” and “Skin friction coefficient” have been set based on comparison of experiments and numerical analysis, see Chapter 3.3, and the specific values can be found in Table 5.

## 2.3 Waves

Waves are a time dependent change in the water elevation and the pressure in the fluid. The pressure below the water surface is in this case normally parted to the static part and the dynamic part of the pressure where the dynamic part of the pressure is a perturbation of the average hydrostatic pressure. Let the wave elevation be described by Airy waves (see e.g. (Airy Wave Theory, 2024)). The water particles will then move in a circular pattern at infinite depth and an elliptic pattern in finite depth as shown in Figure 10.

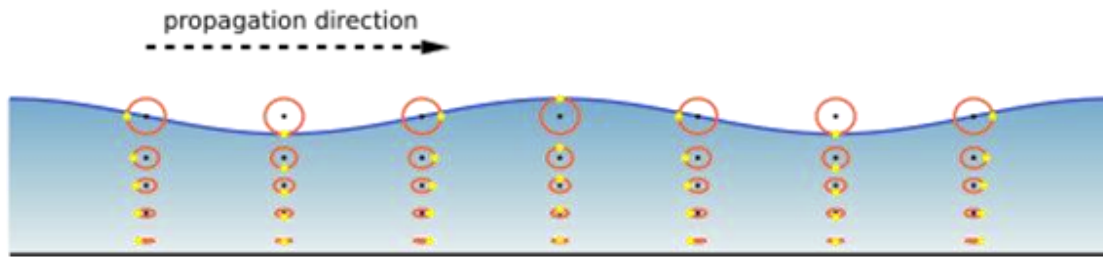


Figure 10 Velocity of water particles under propagating Airy waves

Mathematically wave elevation according to Airy wave theory can be expressed as:

$$\zeta = \zeta_a \sin(\omega t - kx)$$

Equation 14

for waves propagating along the positive x-axis. Waves leads to a time dependent pressure component  $p_d$ . For infinite water depth this is:

$$p_d = \rho_w g \zeta_a e^{kz} \sin(\omega t - kx)$$

Equation 15

where  $\rho$  is density of fluid. For finite water depth, the pressure component is:

$$p_d = \rho_w g \zeta_a \frac{\cosh(z + h)}{\cosh(kh)} \sin(\omega t - kx)$$

Equation 16

where  $k$  is the wave number.  $k = \omega^2/g$  for infinite water depth, and  $k \cdot \tanh(kh) = \omega^2/g$  for finite water depth.

Figure 11 shows pressure under a wave crest and how dynamic pressure and static pressure distributes under a wave crest.

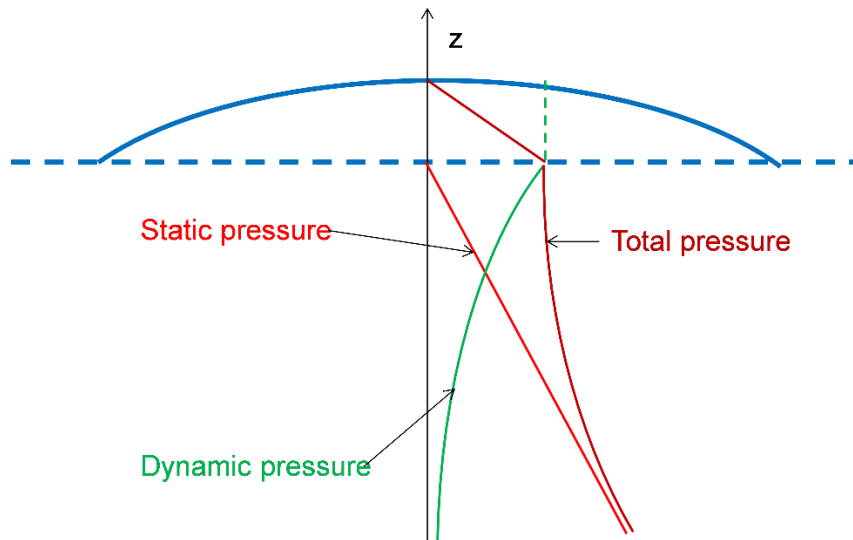


Figure 11 Sea pressure under waves

As seen from Figure 11, the total pressure is the static pressure plus dynamic pressure and can be formulated as:

$$p = p_d - \rho_w g z + p_{atm}$$

Equation 17

Simplified this can be viewed as the hydrostatic pressure under the wave crest, but with the effect of the wave decaying with depth. In the area above the mean water line and under the wave crest, the pressure is calculated simply as the hydrostatic pressure under the instant wave crest. Figure 12 shows the pressure distribution under a wave trough. The static pressure is added to the dynamic pressure, and if the total pressure is less than 0, the surface is out of water and the dynamic pressure is set to the negative of the static pressure so that the total pressure is 0.

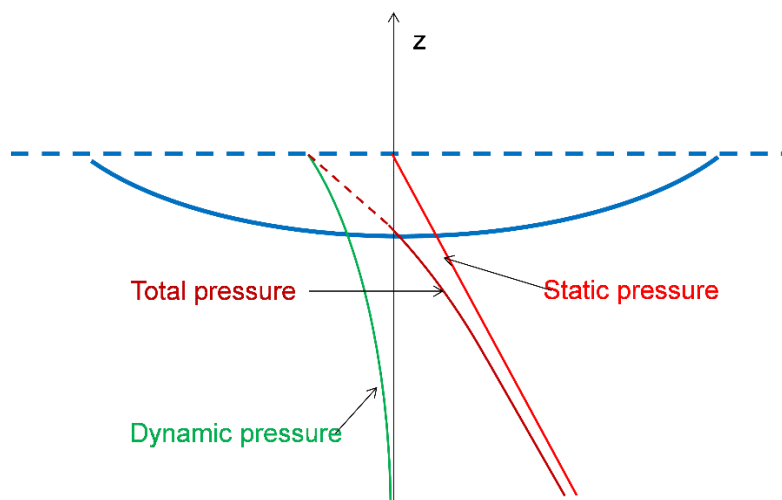



Figure 12 Pressure under wave trough

TR-FOU-2328-5			
			Page 15 of 42
Author: HNM	Verified: AJB	Revision: 9	Published: 08.10.2024

### 2.3.1 Hydrodynamic forces to a stiff body

Consider a body submerged in water under waves, as seen in Figure 13.

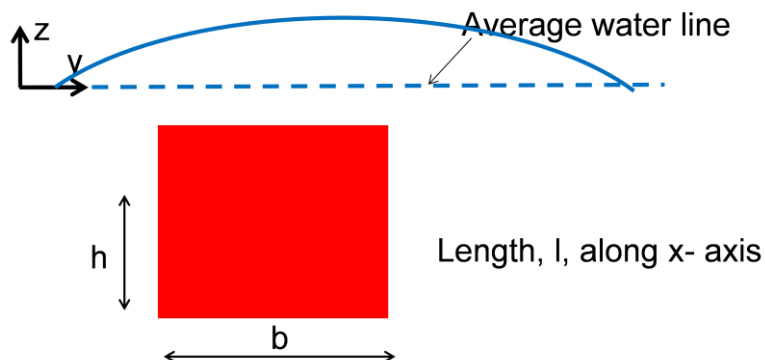


Figure 13 Submerged body

Hydrodynamic forces are forces originating from waves and can be considered a perturbation to the hydrostatic forces. In this section current is neglected. Current influence the total water pattern and hence forces. So do viscous effects which also are neglected in the wave diffraction theory presented in this section.

For practical purposes the hydrodynamic forces are subdivided into a Froude-Krylov term and a diffraction term, where the Froude-Krylov term is force due to the undisturbed pressure field, and the diffraction term is force due to that the object/body changes/disturbs this pressure field.

The boundary conditions being solved are such that the Froude Krylov and the diffracted waves summed satisfy the applicable boundary condition to the body.

Then waves and pressure field caused by body motion is derived and introduced as damping and added mass.

#### *Froude Krylov force*

Forces from water to a submerged body will be integral of the pressure around the body. As the static pressure is constant, we may integrate the pressure to find the force on the body. We start out with integrating the pressure over the surface, then the Froude Krylov force  $F_{FK}$  is:

$$\vec{F}_{FK} = - \iint_{SW} p \vec{n} ds$$

Equation 18

where  $p$  is the pressure introduced by the undisturbed wave field,  $\vec{n}$  is the normal vector pointing outwards, and  $SW$  is the wetted surface.

### *Diffraction force*

The pressure under the waves is associated with fluid velocity. This means that to keep its position, the body in water will introduce a change in the fluid particle motion on and around the body. For a fixed body, the fluid velocity must be zero normal fluid velocity to the body as shown in Figure 14. The forces caused by the pressure of the undisturbed incident waves are called the Froude Krylov forces. The presence of the body is disturbing the incident waves. The forces caused by the body's disturbance of the wave field is called "diffraction forces" and is denoted  $F_D$ . The normal velocity to the body for the diffracted wave field is at any time opposite to the velocity caused by the incident wave.

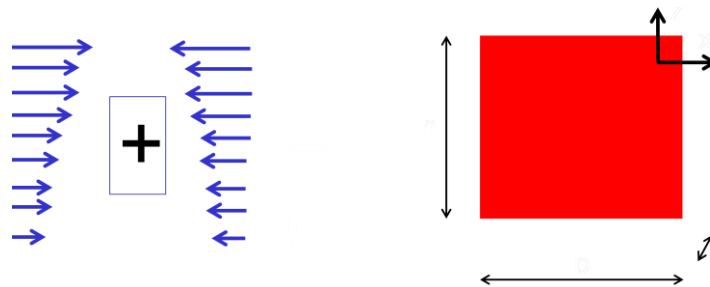


*Figure 14 Velocity field around a submerged body*

$$\vec{F}_D = - \iint_{SW} p \vec{n} ds$$

*Equation 19*

The total force on the body is then:

$$\vec{F} = \vec{F}_{FK} + \vec{F}_D$$


*Equation 20*

Diffraction forces are calculated either by the (MacCamy & Fuchs, 1954) analytical solution or numerically.

MacCamy Fuchs theory is appropriate for vertical cylinders in water where it gives an analytic estimate for the forces acting under the assumption the validity of the method. Application of this to impermeable nets have been outlined in (Berstad & Heimstad, MARINE 2015).

The numerical calculation for derivation of diffraction forces is based on "sink-source" analysis. This means that the object is subdivided to flat plates where there is a source located at each plate. The numerical boundary condition is that this source "blows out" the same amount of water in the opposite direction to counter the water transport through the plate estimated by the Froude Krylov wave theory. This makes it such that the total fluid velocity normal to the plate is 0. For details see e.g. (Babarit & Delhommeau, 2015).



TR-FOU-2328-5			 Page 17 of 42
Author: HNM	Verified: AJB	Revision: 9	Published: 08.10.2024

In AquaSim the panels align with the element panels being impermeable nets of shell elements.

The pros for using numerical calculation of the diffraction forces are that it can cover general geometry. The cons are that there are a large amount of numerical issues that can occur for the numerical calculations. Hence it is of large importance to verify the response parameters seen in AquaView to check the validity of the estimated response.

To describe one such possible origin for numerical issues is that in the analysis a sink-source is blowing water also to the inside of the body, and if the period is close to e.g. sloshing period this can give singularities/resonance effects in the solution making the results unphysical and invalid.

The reason this is not included is that contrary to stiff objects being modelled, the objects modelled in AquaSim are “soft” objects where the velocity and acceleration can be different for different parts. This also means that the diffraction theory may not be a good predictor for loads. The more flexible the response is the less diffraction there will be. This must be carefully evaluated by the engineer.

## 2.4 Hydrodynamic force to a flexible tarpaulin

Consider a fully flexible body following the water particle motions associated with the waves. Consider this applied to a part of a mesh where the waves on the outside of the mesh is assumed to follow the pressure distribution in wave according to linear wave theory. Assuming that in the calculation it is calculated dynamic pressure to one side of a panel and assume a solution where the panel is assumed to follow the flow motion perfectly. This will be like a “free tarp” in water.

In an analysis where the load is distributed to one of the sides of the panel, The load to the panel will, according to airy wave theory for deep waves, be:

$$\vec{F}_{FK} = \rho_w g \zeta_a e^{kz} \sin(\omega t - kx) \vec{n} A$$

*Equation 21*

where  $\vec{n}$  is a vector normal to the plane of the mesh plate. Let’s assume that this is the load applied and that we would like to derive a response where the panel follows the water particle motions of the wave like a “free tarp”. The dynamic response equation is applied such that the response can be derived by the harmonic equation:

$$F = K\eta + C\dot{\eta} + M\ddot{\eta}$$

*Equation 22*

The surface elevation of the incident wave is described by:


$$\zeta = \zeta_a \sin(\omega t - kx)$$

*Equation 23*

And the horizontal part of the water particle velocity is given as:

$$\dot{u}_{xw} = \zeta_a \omega e^{kz} \sin(\omega t - kx)$$

*Equation 24*

TR-FOU-2328-5			
			Page 18 of 42
Author: HNM	Verified: AJB	Revision: 9	Published: 08.10.2024

Furthermore, assuming that there is no mass and no stiffness, the horizontal equation of motion can be described by  $F_1 = C_1 \dot{\eta}_1 A_x$ . By assuming that the response is equal to the horizontal water particle velocity  $\dot{\eta}_1 = \dot{u}_{xw}$ , and having,

$$F_1 = F_{FK} = \rho_w g \zeta_a e^{kz} \sin(\omega t - kx) A_x$$

Equation 25

a solution for the damping  $C$  is found:

$$C_1 = \rho_w g / \omega$$

Equation 26

This will lead to a horizontal response of the panel that moves along with the horizontal water particle motion of the waves, given that the panel is oriented perpendicular to the wave direction. This means that for a “free tarp” with a vertical side where the waves approach normal to the side, introducing Equation 26 as a damping term will lead to a response, where the tarp follows the horizontal motions of the wave particles, if no other forces are acting. For the vertical direction, the water particle motion is described by:

$$u_{zw} = \zeta_a e^{kz} \sin(\omega t - kx)$$

Equation 27

where  $K = \rho_w g$ , will lead to a possible solution. This is added as stiffness in the vertical direction. It is not good to base a solution on stiffness since there is no related work, hence we rather consider the vertical water particle velocity, given by:

$$\dot{u}_{zw} = \zeta_a \omega e^{kz} \cos(\omega t - kx)$$

Equation 28

Meaning that for the solution in Equation 26 to be applicable vertically, i.e.  $C_3 = C_1$ , a force corresponding to the Froude Krylov force in Equation 21 must be set to Equation 29 instead.

$$F_{FK} = F_3 = \rho_w g \zeta_a e^{kz} \cos(\omega t - kx) A_z$$

Equation 29

As an option, damping in the vertical direction can be chosen to be different than in the horizontal direction, but 1 is consistent with a tarp following the water particle motion in the direction normal to the panel.

## 2.5 Added mass and damping

### 2.5.1 Hydrodynamic added mass and damping

The numerical solution from the hydrodynamic analysis also proposes added mass and damping from a distribution calculated numerically. Using coefficients of 1.0 means these parameters are used as proposed. They can be scaled by changing these parameters. The added mass and damping should be evaluated by the engineer.

When the MacCamy Fuchs formulation is applied, the added mass and hydrodynamic damping is based on coefficients relating to the radius of the element to the centre point of the panels representing the object.

## 2.5.2 Notes on damping

With respect to damping, it can be introduced both through “Hydrodynamic damping”, or “Damping” according to Equation 24. These are added for the total damping. In addition, Rayleigh damping and damping in the Newmark Beta methodology are damping that may be introduced. The end user must keep track of the total damping compared with knowledge of how large the damping should be. Figure 15 shows added mass and damping for the structure seen in the same figure.

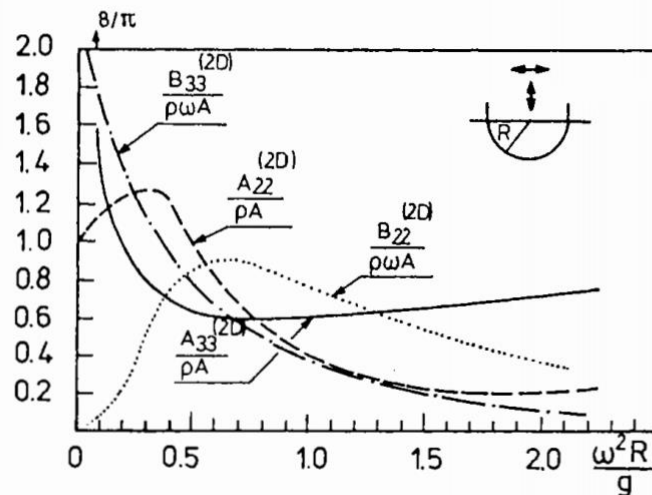


Fig. 3.6. Two-dimensional added mass and damping in heave and sway for circular cylinder with axis in the mean free-surface. Infinite water depth. ( $A_{22}^{(2D)}$  = added mass in sway,  $B_{22}^{(2D)}$  = damping in sway,  $A_{33}^{(2D)}$  = added mass in heave,  $B_{33}^{(2D)}$  = damping in heave,  $\rho$  = mass density of water,  $A = 0.5\pi R^2$ ,  $\omega$  = circular frequency of oscillation).


Figure 15 Added mass and damping for a cylinder in water (Faltinsen, 1990)

## 2.6 Wave drift forces

The nonlinearity that arises from the in and out of water is one of the 2<sup>nd</sup> order effects that give rise to drift forces. An overview of this and handling in AquaSim is found in (Aquastructures, 2013).

Note that in the consideration for the wave drift forces waves caused by oscillation of the body is not accounted for. This is because in the analysis bodies are described by many nodes and are in general flexible so that “stiff body motion” is not a valid expression. This means that engineers must evaluate this carefully. The reason this is not included is that contrary to stiff objects being modelled, the objects modelled in AquaSim are “soft” objects where the velocity and acceleration can be different for different parts. This also means that the diffraction theory may not be a good predictor for loads. The more flexible the response is the less diffraction there will be. This must be carefully evaluated by the engineer.

When drift is turned on, also the pressure caused by the velocity term of the Bernoulli equation is accounted for (Aquastructures, 2016) is included such that all terms leading to drift is included (being in and out of water and this term).

TR-FOU-2328-5			 Page 20 of 42
Author: HNM	Verified: AJB	Revision: 9	Published: 08.10.2024

## 2.7 Hybrid load model

The hybrid load model is an option to use which can be applicable for cases between the cases of stiff structure and flexible systems. When the hybrid solution is used, loads are based on one part from the flexible tarp formulation and the other part from the MacCamy Fuchs (MF) or numerical diffraction (NUM) solution. The user decides how much each part accounts for. If as an example scaled factor is 0.3, 30% of the loads are based on the MF or NUM model while 70 % of the loads are calculated from the free tarp formulation in section 2.4.


## 2.8 In and out of the waterline

At each timestep, the waterline is kept track of, including the wave elevation corresponding to the pressure from the diffracted wave. At each time instant, total pressure consisting of the pressure caused by waves and the hydrostatic pressure is calculated, and if this pressure is less than zero, the pressure is set to zero.

## 2.9 Waves and current combined

Combining waves and current, the following assumptions apply:

- Waves are assumed to “ride” on top of the current field.
- In case of varying current as function of depth, waves will ride on top of the current velocity at  $z = 0$ .
- For pressures originated by waves there are no adjustments due to current.
- When calculating the relative velocity to generate the pressure seen in Figure 5 in a dynamic state, the relative velocity is calculated at each element, or averaged in horizontal plane based on user choices.

TR-FOU-2328-5			 Page 21 of 42
Author: HNM	Verified: AJB	Revision: 9	Published: 08.10.2024

## 3 Case studies

As set of case studies has been analysed to check the validity of results.

### 3.1 Vertical stiff cylinder

The Morison equation reads:

$$F = \rho_w V \dot{u} + \rho_w C_a V \dot{u} - \rho_w C_a V \dot{v} + \frac{1}{2} \rho_w C_d A (u - v) |u - v|$$

*Equation 30*

where  $C_a$  is the added mass coefficient and  $C_d$  is the drag coefficient. These are parameters set empirically or analytically. Description can be seen at (Morison equation, 2024). The terms in Equation 27 are:

- $\rho_w V \dot{u}$  is the Froude Krylov force. This term is added not only in the z-direction, but also for the horizontal plane as well.
- $\rho_w C_a V \dot{u}$  is the diffraction force. I.e., related to the calculated diffraction of waves.
- $\rho_w C_a V \dot{v}$  is the added mass.
- $\frac{1}{2} \rho_w C_d A (u - v) |u - v|$  is the drag force.

$V$  is submerged volume,  $A$  is area fronting the fluid flow. Set the viscous drag coefficient to 0, and consider a cylinder, can be written as:

$$F = \rho_w V \dot{u} + \rho_w C_a V \dot{u}$$

*Equation 31*

where the first term is due to the Froud Krylov force, and the latter term is due to the diffraction force. The analytic case says  $C_a = 1$  meaning:

$$F = 2\rho_w V \dot{u}$$

*Equation 32*

The Morison Equation solution in Equation 32 should be found also in an analysis for a fixed object given that the velocity predicted by the incident wave in the centre of the object,  $\dot{u}$ . A test case with a cylinder as seen in Figure 16 has been established.

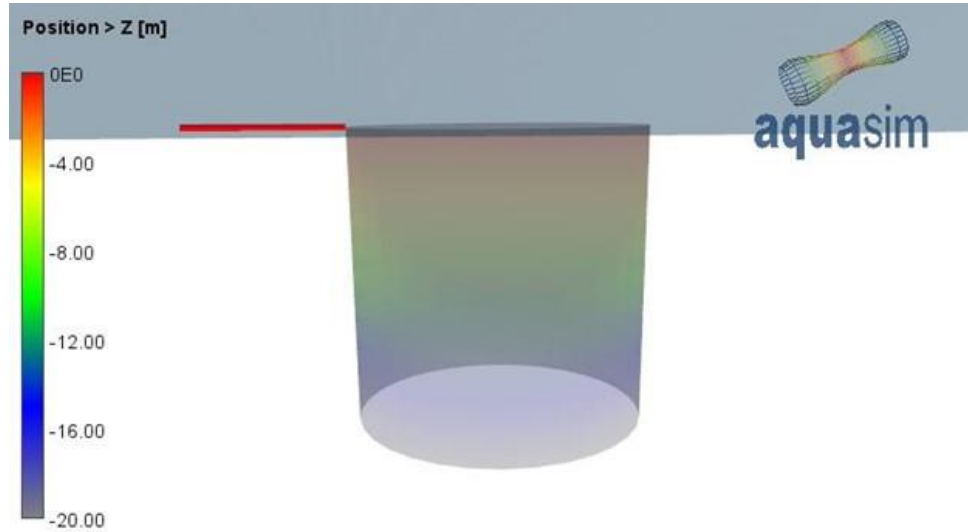


Figure 16 20-meter-deep cylinder with diameter 20 meter. Depth of objects are indicated by colour. On top there is a truss element which is fixed on the left end

The cylinder in Figure 16 is withheld from motions except in the x-direction meaning that all forces in the wave direction must be distributed through the truss element. 320 elements/panels are distributed to the cylinder as seen in Figure 17. There are 32 panels along the circumference and 10 panels in the vertical direction. A refined analysis model has been established with 64 elements/panels along the circumference and 20 panels downwards.

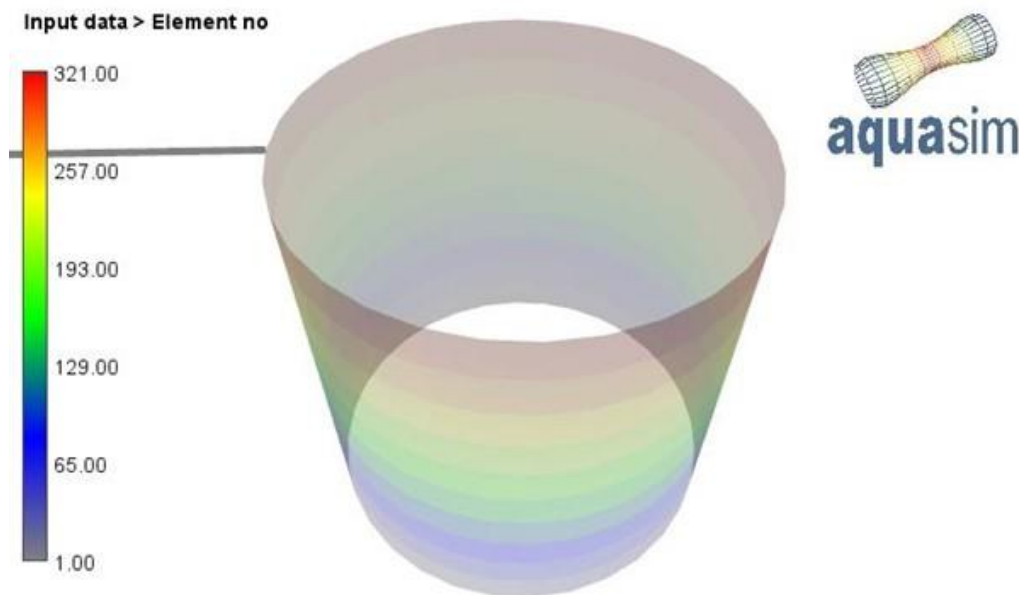


Figure 17 Elements and panels on the cylinder

Figure 18 shows results where the long wave theory is compared to results calculated by AquaSim using two different methods/models:

- AquaSim MacCamy Fuchs – In this case wave diffraction is calculated from the MacCamy Fuchs solution.
- AquaSim Numerical – In this case the numerical method is used to calculate diffraction.

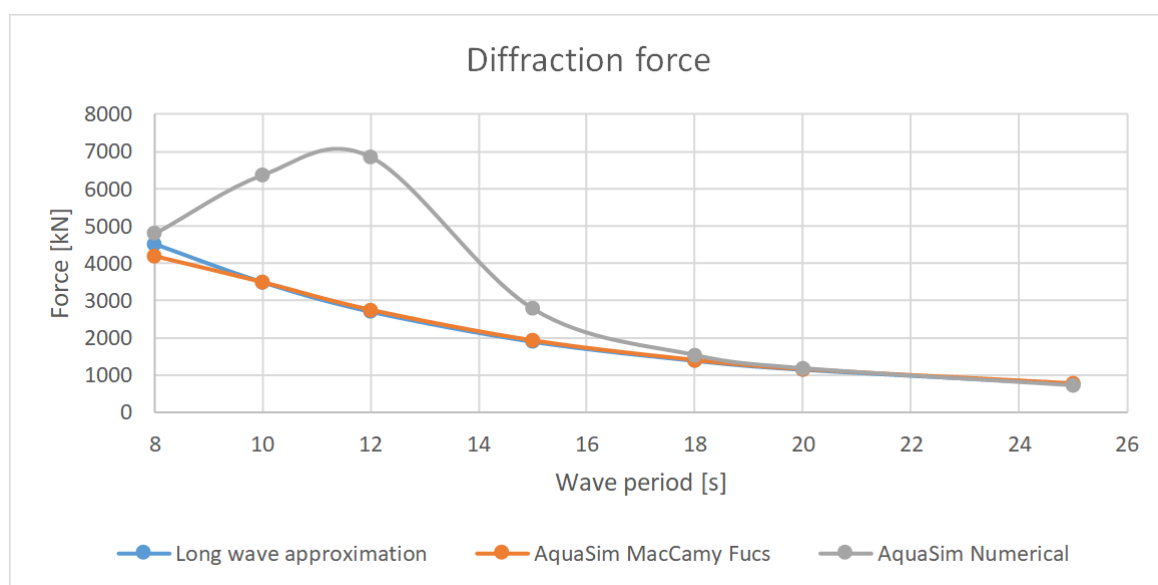


Figure 18 AquaSim results compared to long wave theory

As seen, there is a good correspondence between the long wave theory and the MacCamy Fuchs analysis results. The results for the numerical analysis do not compare as well for some wave periods. In general aspect to be aware of considering numerical analysis:

- There might be errors in the numeric calculations.
- The theory may not reflect the modelled system.
- There might be resonance effects in the prediction. For instance, this could be a type of sloshing period. In this case there is a sloshing period for a shallow tank at period 12 sec. Since the tank is bottomless it can also be numerical effects from that as well.
- Diffracted wave may not have been found and is then set to zero.
- Since AquaSim is not interested in artificial results, the amplitude of diffracted waves larger than 1 is set to 1. This means that unphysical effects may be dampened. Hence the results should be evaluated, and load model carefully chosen based on such considerations.

AquaView have tools to evaluate certain response parameters. Parameters are seen in Figure 19.

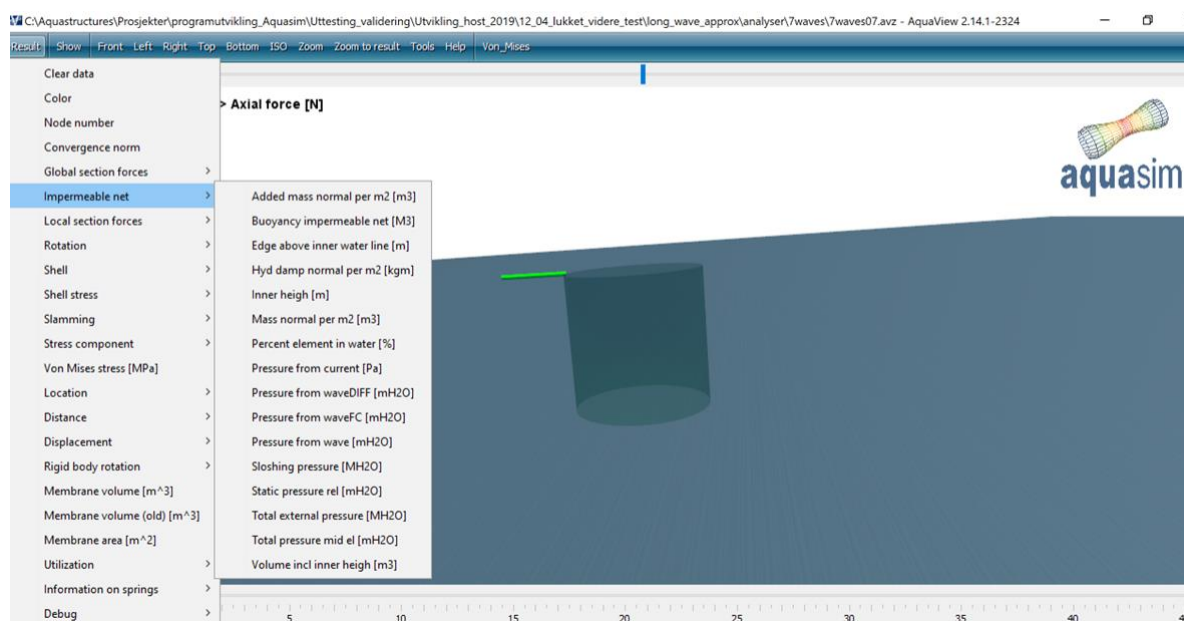


Figure 19 Response parameters for General impermeable net

Note also that response parameters such as diffraction and added mass are based on the response from a stiff body. As discussed, this is not applicable for a fully flexible body, and for partly flexible bodies, the scaled diffraction option may be considered and is evaluated for a case in section 3.3.

### 3.2 Case compared to reflection from wall

Figure 20 shows a case with a wall, 5 meters thick and 20x20 wide and deep. For short wave lengths one may assume that the wave to a wall solution should correspond with analysis results.

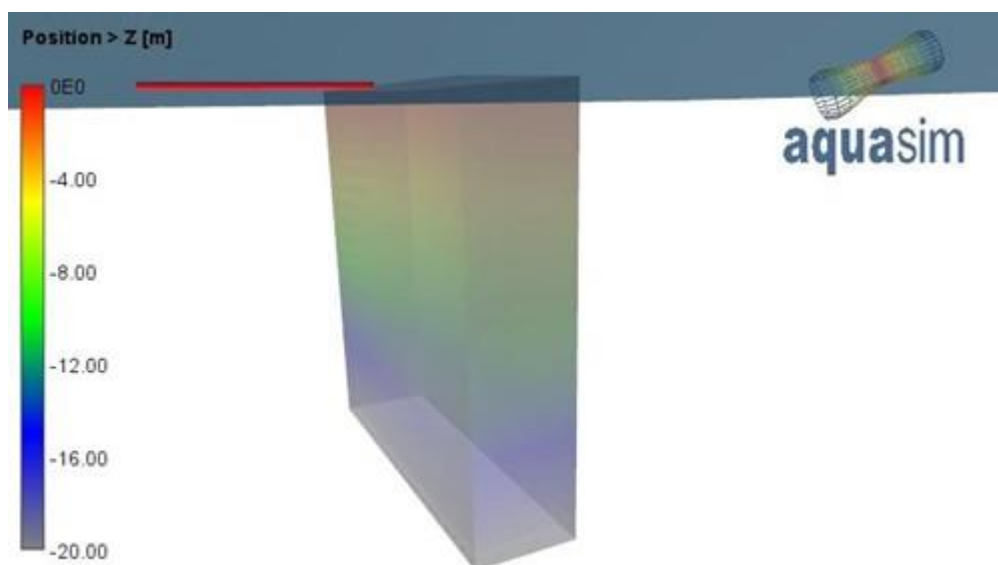


Figure 20 Test case 20x20 m wall, 5 meter thick



The model has 20x20 elements on each main side and elements 20 elements connecting the front and back sides and bottom as seen in Figure 21.

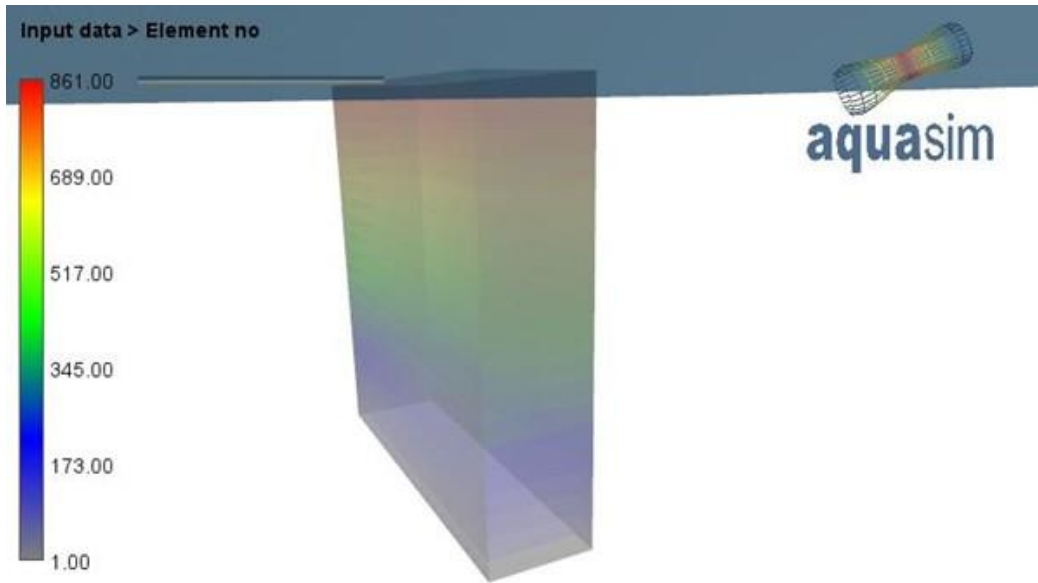


Figure 21 Elements in analysis model of square sections

The analysis model is only allowed to move along the x- axis and is withheld on the node to the left of the truss such that all forces will be seen in terms of axial force in the truss. Figure 22 shows results from AquaSim compared to an analytic solution based on the “standing wave” approximation. In this case only the numerical method is used in AquaSim.

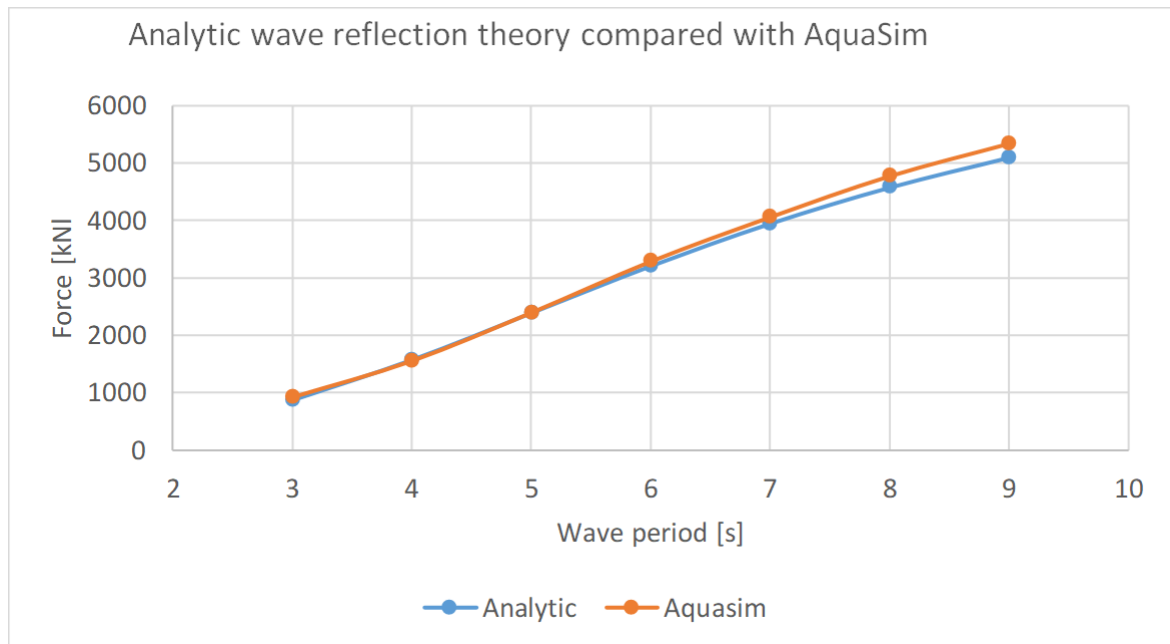


Figure 22 Comparison of analytical formula to numerical solution

As seen from Figure 22, the results compare well for this case.

### 3.3 Flexible tube net

A flexible tube net as shown in Figure 23 have been analysed with AquaSim 2.19.1. The AquaSim model is shown in Figure 24.



Figure 23 Deformed net (Egersund Net, 2020)

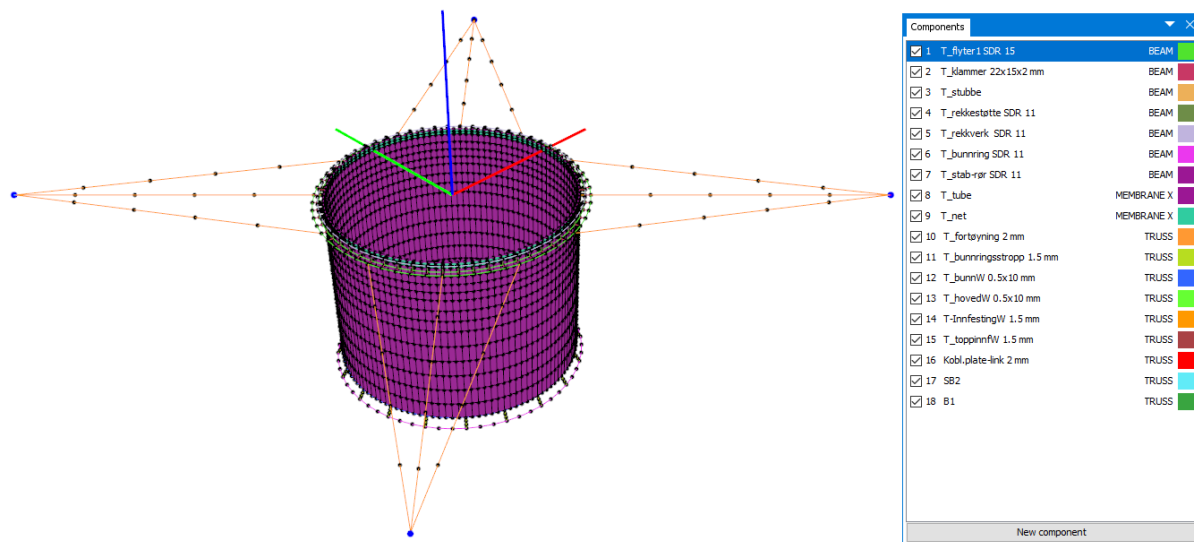


Figure 24 Analysis model of tube in AquaSim

Figure 25 shows the analysis model in model scale with the colours showing the vertical location. The coordinate system follows the AquaSim defaults with the z-axis pointing upwards and  $z = 0$  is in the still water line.

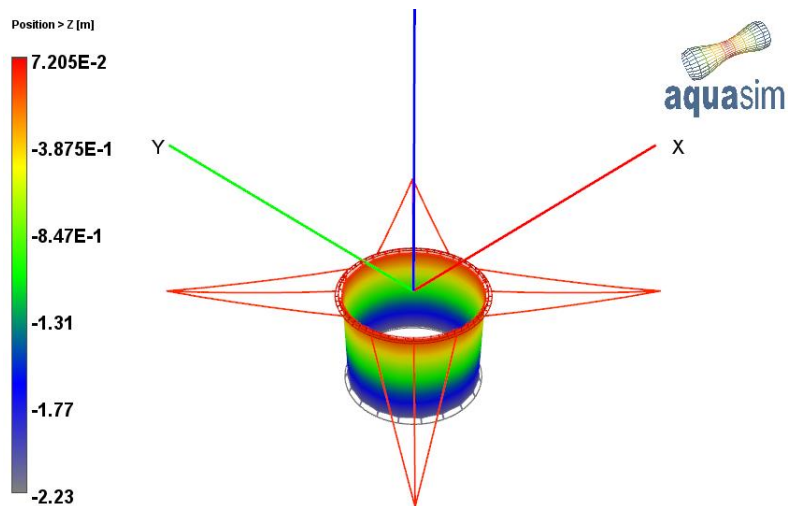


Figure 25 Tubenet. Colours shows vertical location in static equilibrium

Loads are measured in terms of axial force in bridles. In the Tubenet-model, the bridles are coupled through one end-piece, as shown in Figure 26. Forces from all bridles goes through this end-piece. This corresponds to the location of the load-cell in the tank test.

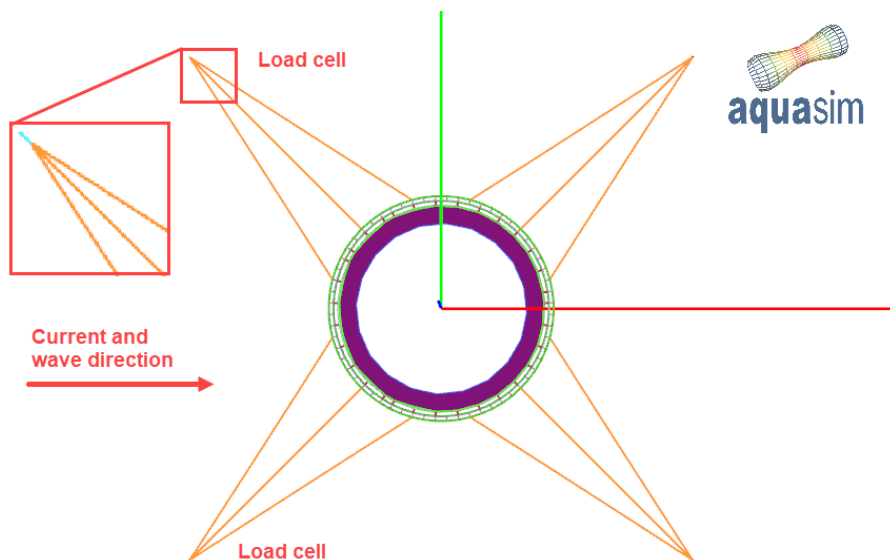


Figure 26 Bridles coupled through one endpiece which is the load cell in the model test. Forces from all bridles goes through the load cell both in the model test and in the analysis

The analysis model is double symmetric. Figure 27 shows transverse (y-) location of the system. As seen from the figure, the model is 7 meters wide. The water depth of the tank is 2.7 meters and the width of the tank is 8 meters. Tank and effects from tank walls are not included in analysis.

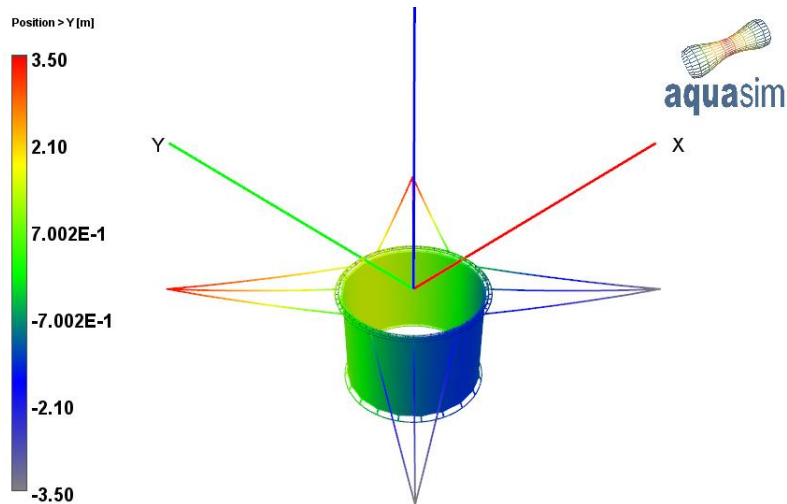


Figure 27 Transverse (y) position of Tubenet and bridles

### 3.3.1 Testing and comparison current

Three current-cases are tested in the tank and correspondingly simulated in AquaSim.

Figure 28 shows the tube exposed to 9.7 cm/s current, Figure 29 shows the same with 14.5 cm/s current and Figure 30 for 19.3 cm/s. Figure 31 shows the condition of 19.3 cm/s from a bird view.

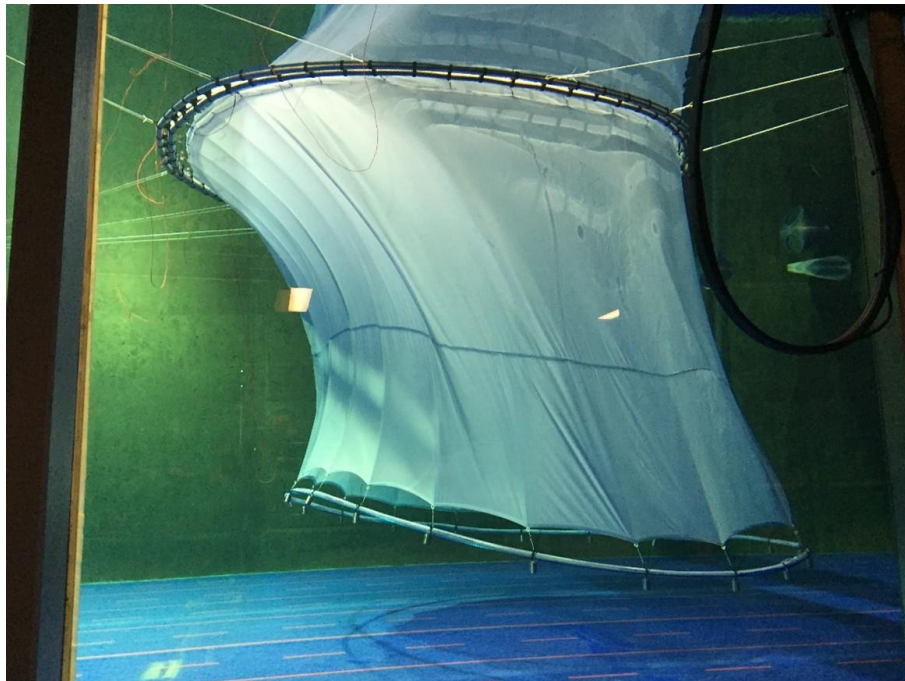


Figure 28 Tubenet exposed to 9.7 cm/s current

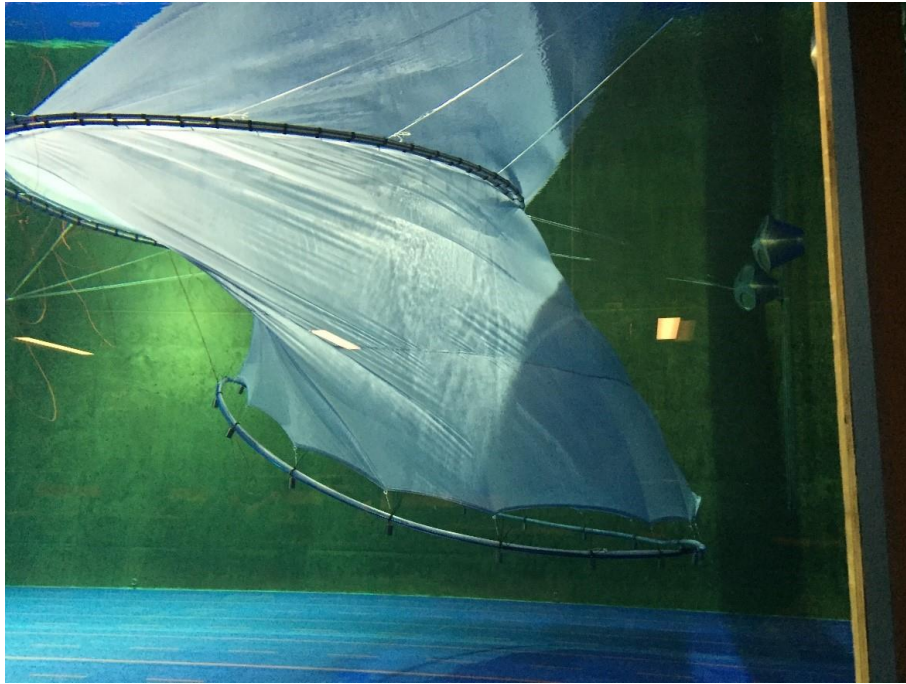


Figure 29 Tubenet exposed to 14.5 cm/s current

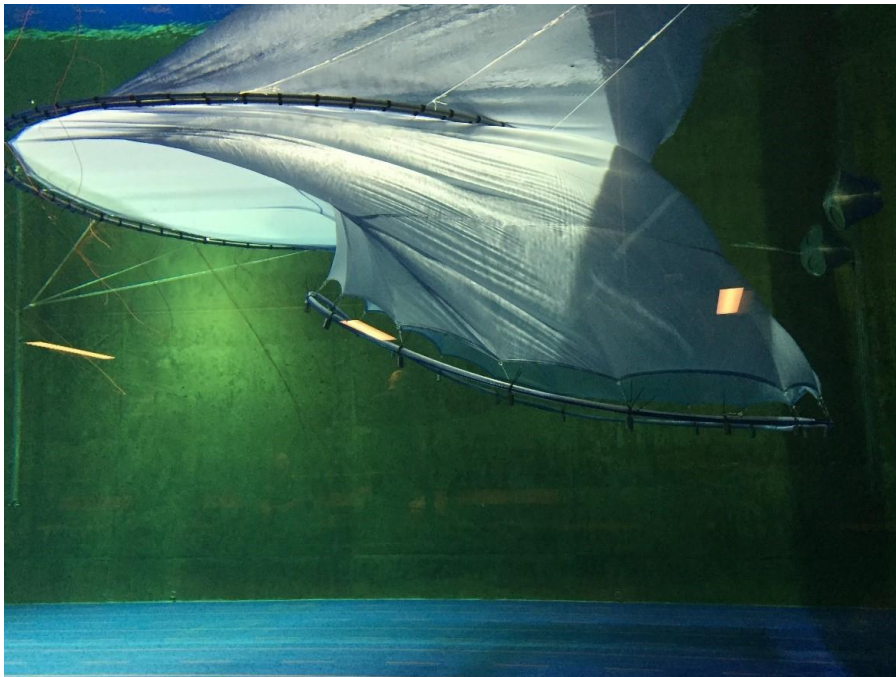


Figure 30 Tubenet exposed to 19.3 cm/s current

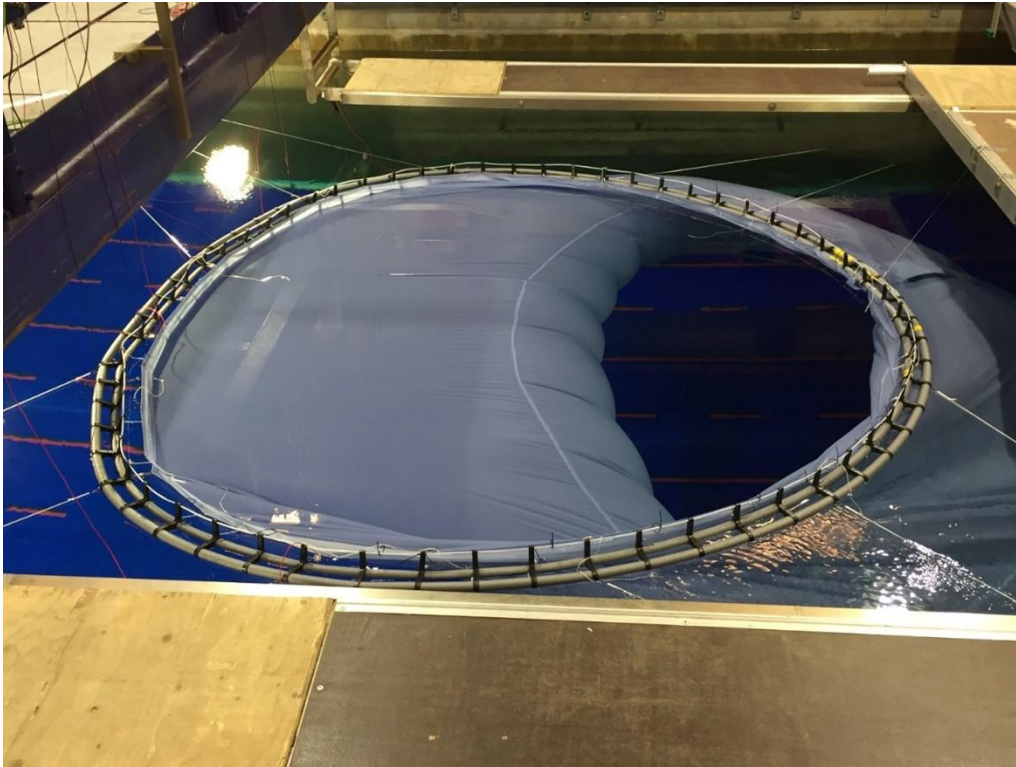


Figure 31 Tubenet exposed to 19.3 cm/s current (bird view)

As seen from Figure 28-Figure 31, the tube deforms strongly, in particular from 14.5 cm/s current velocity. This means one cannot assume the pressure around a cylinder to be the valid pressure-formulation for the pressure-distribution and total drag. However, as the pressure distribution varies with the coefficients in the equations, and that the cross-flow method is part of the general formulation one can assume to be in the 'ballpark' when comparing results.

Before comparing to analysis, the following should be noted from the tank test:

- It is seen that the part of the tube upstream moves more upwards than the part downstream.
- The water tank has closed volume meaning the water pumped through the tank must pass through. As seen from Figure 28-Figure 31 in particular the bottom is close to the tube. The bottom ring of the tube is 2.2 m deep and the tank is 2.7 meters deep (SINTEF, 2020). This may be of larger importance for 14.5 cm/s and 19.3 cm/s since as seen from Figure 28-Figure 31 the tube deforms such that most of the water seems to go under the tube and not around. For a node-formed net, the relation between the transverse area the flow is passing through where there is no net and the area where the tube is given in Table 2.


TR-FOU-2328-5			 Page 31 of 42
Author: HNM	Verified: AJB	Revision: 9	Published: 08.10.2024

Table 2 Transverse area of tank and tube

<b>Transverse area tank [m<sup>2</sup>]</b>	21.60
<b>Transverse area tube [m<sup>2</sup>]</b>	6.05
<b>Transverse free flow area [m<sup>2</sup>]</b>	15.55
<b>Factor</b>	1.39

As seen from Table 2, the water need to increase velocity by approximately 40 %, assuming undeformed geometry, to maintain the same flow rate around and under the tank. As the tube deforms, the tube blocks a lower part of the transverse area, but in this case more flow is lead under the tank where the clearance is lower such that for comparing test and analysis. As an approximation, the results have been placed at two points where the first point is the nominal velocity and the second is the velocity multiplied with 1.4.

The load cells have been placed in each side of the upstream bridles as seen in Figure 26. The load cells collect all the forces in the three bridles. Loads are symmetric between the bridles. Axial forces from the AquaSim analysis are collected from the load cell-point highlighted in Figure 26.

Figure 32 shown a comparison of results between model test and analysis. The following applies to this figure:

- The yellow lines represent measurements in the tank, “Experiment”. The mark to the left of the test result at the nominal velocity while the right mark represents a simplified upper bound by estimating how much the velocity needs to be increased to account for a factor of 1.4 due to the finite cross section in the transverse plane.
- The results labelled “Experiment (test)” is results from one of the load cells indicated in Figure 26.
- MH2O is the unit “Meters of water” where 1 Bars = 10.1974 Metres of water.

The analysis has been carried out with the parameters given in Table 3. The lift coefficient  $Cl$  has been varied with three different values.

Table 3

Parameter	Abbreviation	Value
Drag coefficient upstream	$C_{d\ UPSTREAM}$	1
Drag coefficient downstream	$C_{d\ DOWNSTREAM}$	0.5
Lift coefficient	$Cl$	3, 1 and 0.1
Skin friction coefficient (tangential drag)	$C_t$	0.02

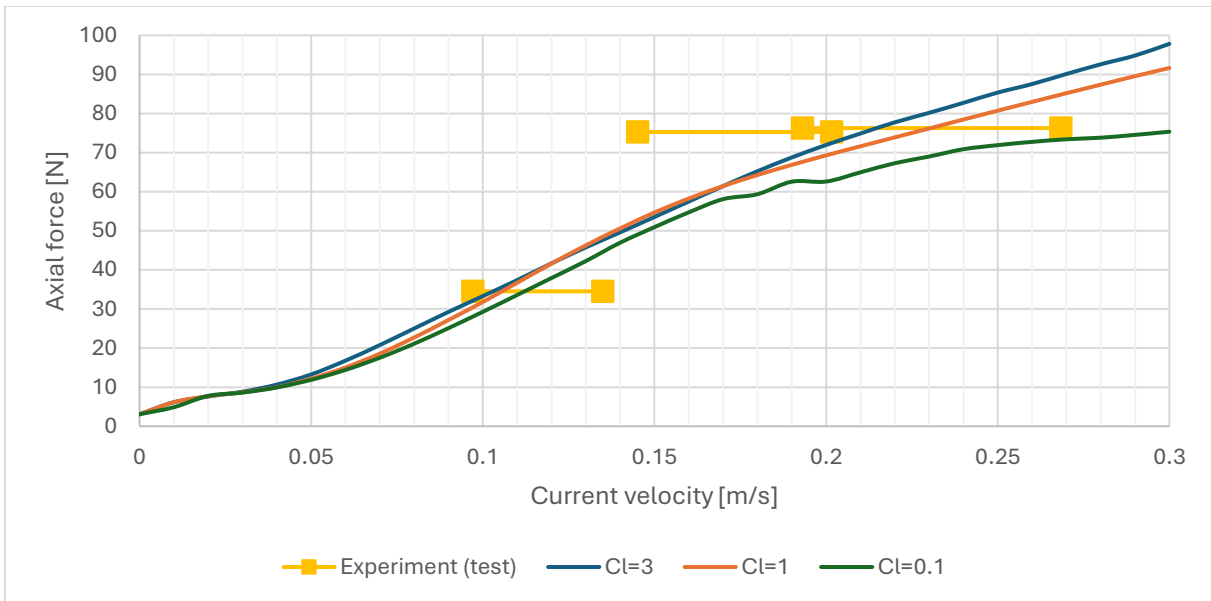


Figure 32 Analysis with varying lift coefficient compared to tank test result (experiment)

Figure 33-Figure 35 shows the response of the system with a lift coefficient of 1. The left side shows a snapshot from the tank test (experiment), the right side shows the corresponding AquaSim analysis.

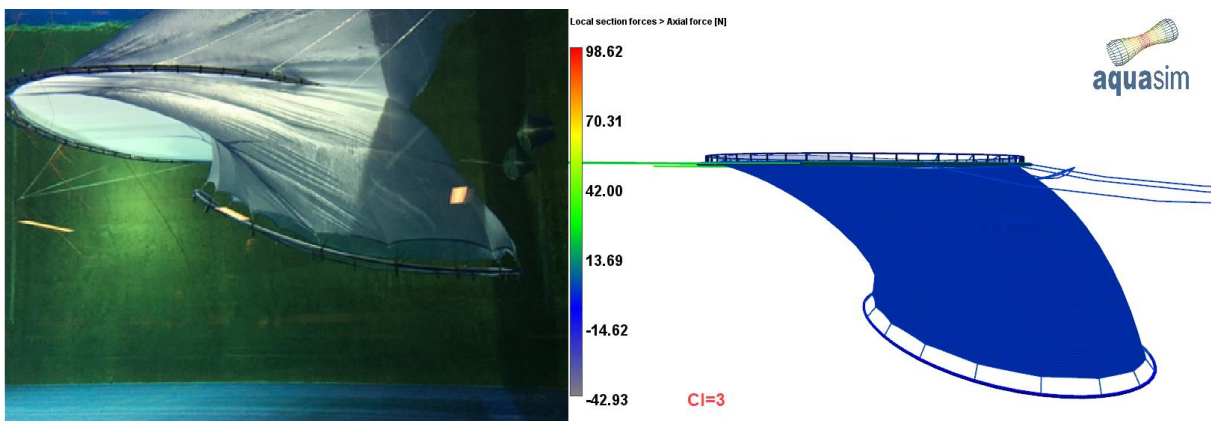


Figure 33 Current velocity 0.193 m/s,  $Cl=3$ .



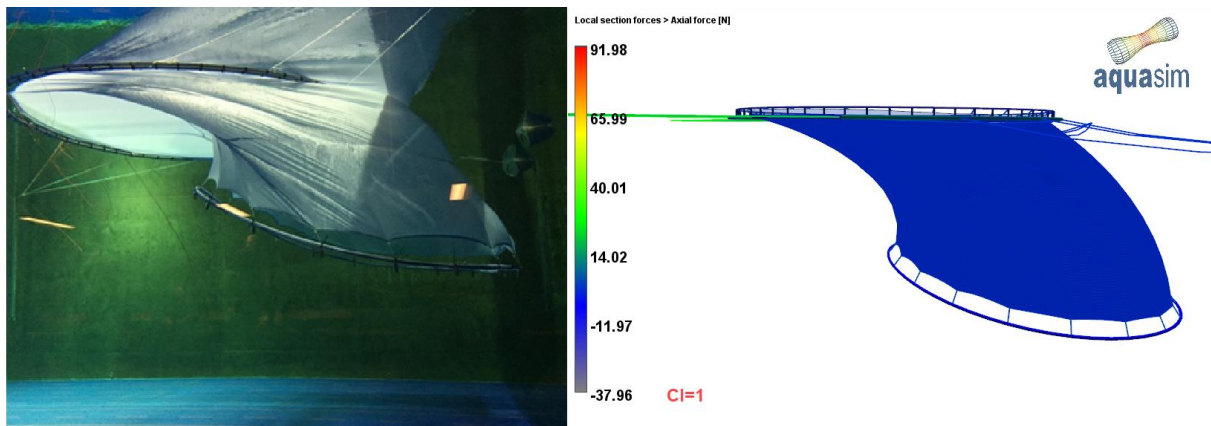


Figure 34 Current velocity 0.193 m/s,  $Cl=1$ .

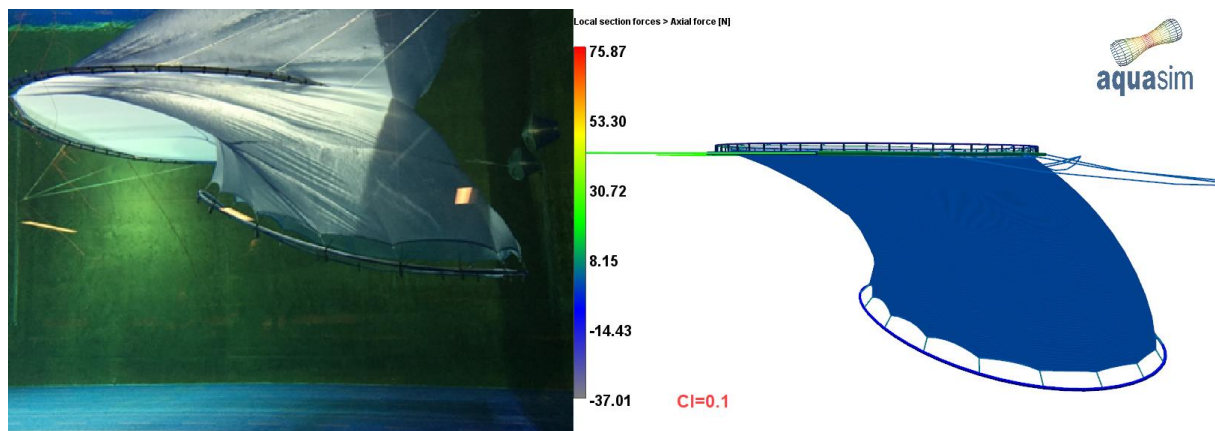


Figure 35 Current velocity 0.193 m/s,  $Cl=0.1$ .

By comparing the graph in Figure 32 with Figure 33-Figure 35 it is found that a lift coefficient of  $Cl = 1$  compares best when the level of axial force and deformations is evaluated. Other analyses (not presented here), show that the axial forces are sensitive for the skin friction (tangential drag), and that lower drag coefficient upstream contributes to some better match with tank test for current velocity of 0.097 m/s. Parameters presented in Table 3 with lift coefficient equal to 1 is used as basis for further analyses.

### 3.3.2 Testing and comparison regular waves with current

Three cases with current and waves are tested in the tank and compared with AquaSim analysis. The current- and wave data for the cases are presented in Table 4

Table 4 Cases with current and waves

	Case 1	Case 2	Case 3
<b>Current velocity [m/s]</b>	0.097	0.145	0.193
<b>Wave amplitude [m]</b>	0.0988	0.0988	0.0988
<b>Wave period, nominal [s]</b>	1.217	1.244	1.271
<b>Wave period earth fixed [s]</b>	1.158	1.158	1.158

Figure 36 shows the response time series of the three tank test cases.

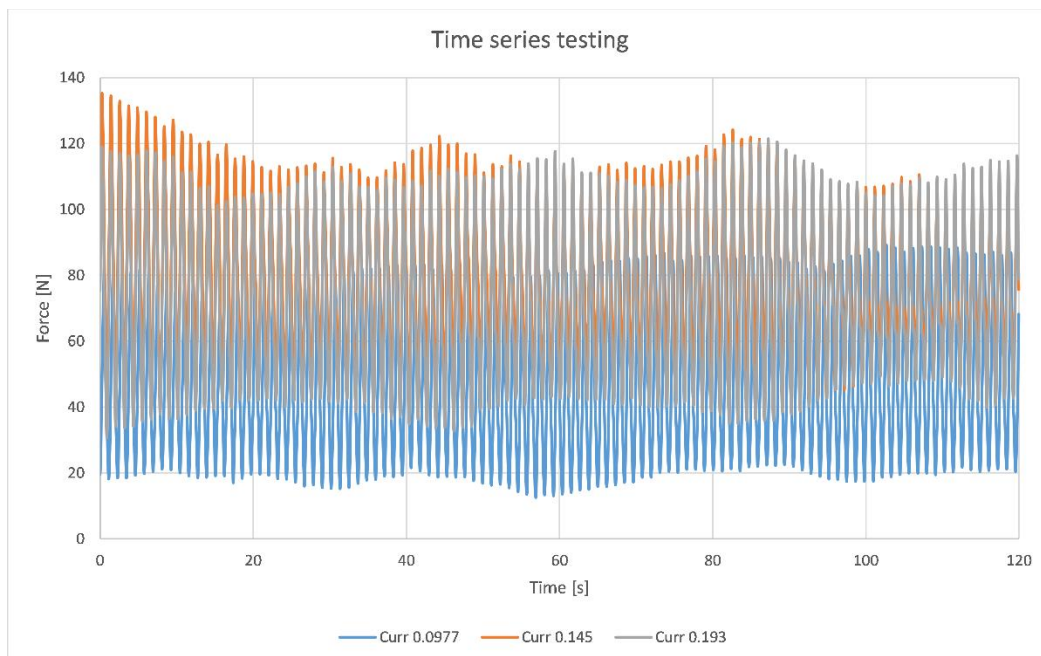


Figure 36 Time series case 1, 2 and 3. The average of the axial load on the left and right load cell on the bridles

Parameters for dynamic analysis in AquaSim are given in Table 5. Each case has been analysed with the available type of diffraction load-formulations in AquaSim.

Table 5 Parameters for the Tubenet-model, dynamic analysis

Parameter	Type of diffraction load						
	Flexible tarp	MacCamy-Fuchs	Hybrid Flexible tarp/ Numerical=0.2	Hybrid Flexible tarp/ Numerical=0.25	Numerical diffraction	Hybrid Flexible tarp/ MacCamy-Fuchs=0.2	Hybrid Flexible tarp/ MacCamy-Fuchs=0.25
Density of fluid inside tank	0	0	0	0	0	0	0
Inner fluid mass scaling	0	0	0	0	0	0	0
Drag coefficient upstream	1	1	1	1	1	1	1
Drag coefficient downstream	0.5	0.5	0.5	0.5	0.5	0.5	0.5
Skin friction coefficient (tangential drag)	0.02	0.02	0.02	0.02	0.02	0.02	0.02
Lift coefficient	1	1	1	1	1	1	1
Added mass coefficient horizontal	0	0.25	0.2	0.25	1	0.05	0.0625
Added mass coefficient vertical	0	0.25	0.2	0.25	1	0.05	0.0625
Added mass indicator	0	0	0	0	0	0	0
Hydrodynamic damping coefficient horizontal	0	0.25	0.2	0.25	1	0.05	0.0625
Hydrodynamic damping coefficient vertical	0	0.25	0.2	0.25	1	0.05	0.0625
Damping coefficient (flexible tarp)	1	1	1	1	1	1	1
Damping coefficient (flexible tarp) tangential to panels	0	0	0	0	0	0	0
Combined pressure from waves and current	1	1	1	1	1	1	1

Note on Damping coefficient (flexible tarp): for simplicity, this parameter is to 1.0 for all diffraction load models, in this case. Otherwise, in AquaSim 2.19.1, for the “Hybrid” diffraction models, the parameters are set, as a default, in a manner such that they are weighted consistently with the default values from the “Flexible tarp” formulation and the chosen diffraction formulation, based on the values set for “Diffraction scaling”. Table 5 is consistent with this, except for the parameter “Damping coefficient (flexible tarp)”, which for simplicity has been set equal to 1.0 for all diffraction load models and has not been weighted.

**Case 1**

Average line tension force in the load cell from the tank test is presented in Figure 37.

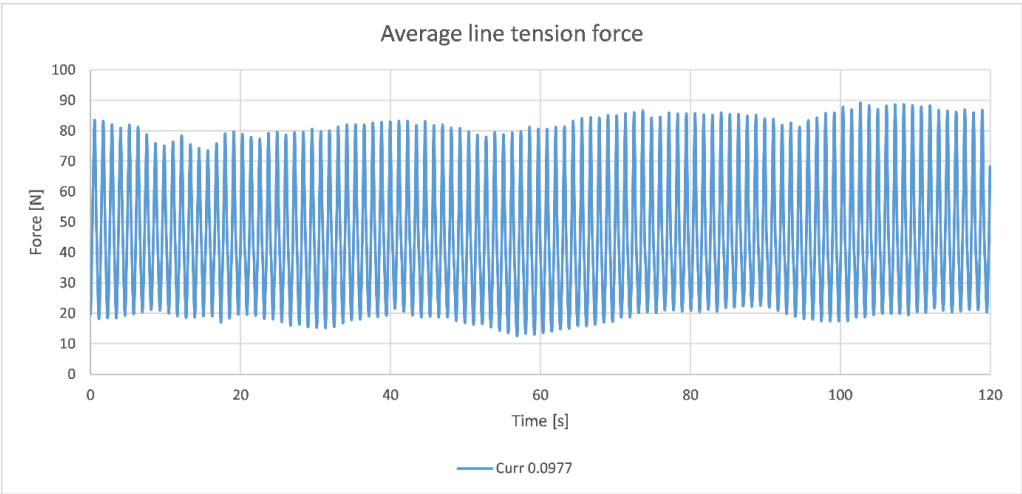


Figure 37 Average line tension force in load cell from tank test

Comparison of experiment (tank test) and AquaSim analysis is presented in Figure 38. “Experiment (Case 1)” are data from the tank test. The other curves are AquaSim analysis results; axial force from the load-cell point, as described in Figure 26.

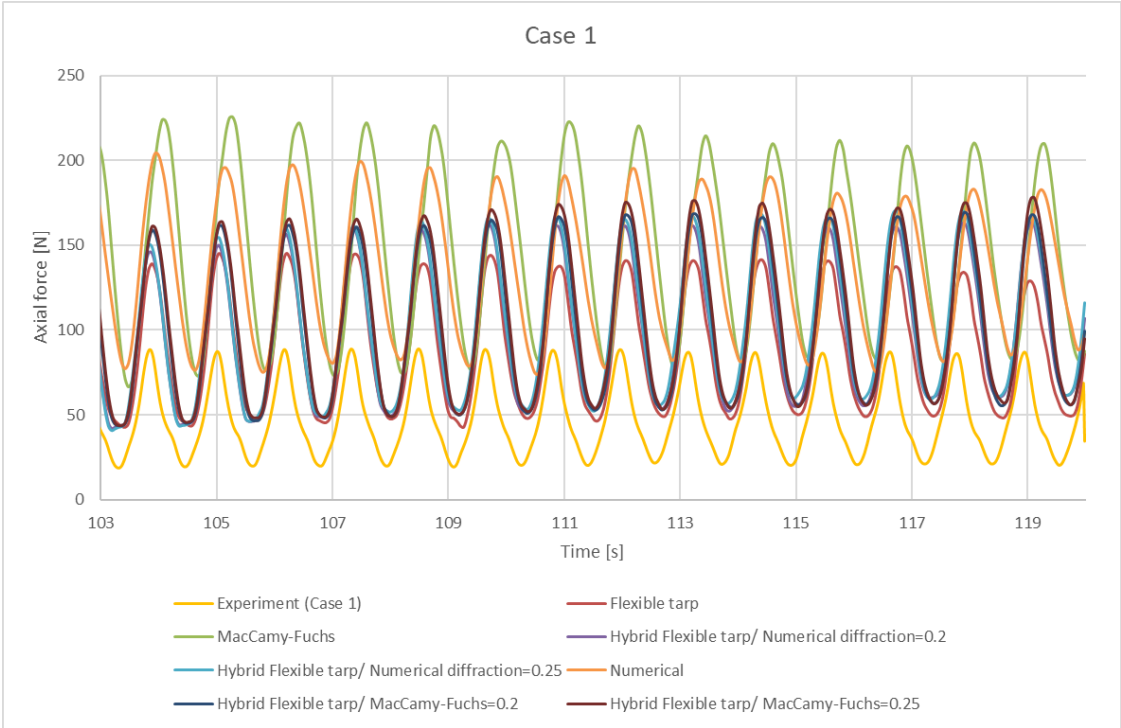


Figure 38 Results Case 1

As seen by comparing analysis and measurements, the results generally compare well. The max values for the AquaSim analyses are generally at higher level than the tank test data. However, the amplitude of the force (difference between max and min values) match well when comparing tank test data and AquaSim. This is believed to be due to Stokes drift velocity. This is a second order effect and is the average velocity of a fluid parcel when it travels with the fluid flow, see e.g. (Wikipedia, 2024d). This type of drift is not seen in the tank test data. In the tank, the flow is constant in terms of amount of water being transported. This mean that since stoke drift leads to water transport, the effective current is lower.

Overall, the AquaSim analysis results are considered to be on the conservative side.

### Case 2

Average line tension force in the load cell from the tank test is presented in Figure 39.

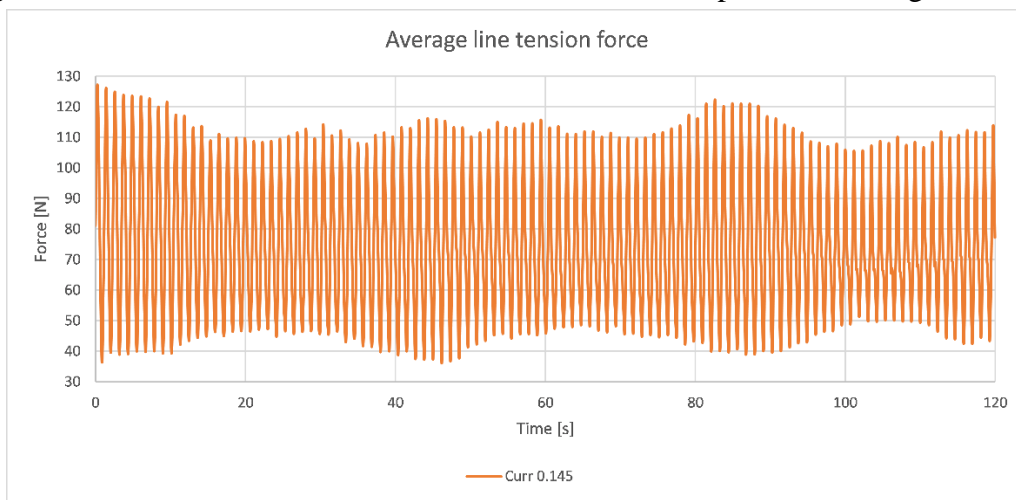


Figure 39 Average line tension force in load cell from tank test

Comparison of experiment (tank test) and AquaSim analysis is presented in Figure 40. “Experiment (Case 2)” are data from the tank test. The other curves are AquaSim analysis results; axial force from the load-cell point, as described in Figure 26.

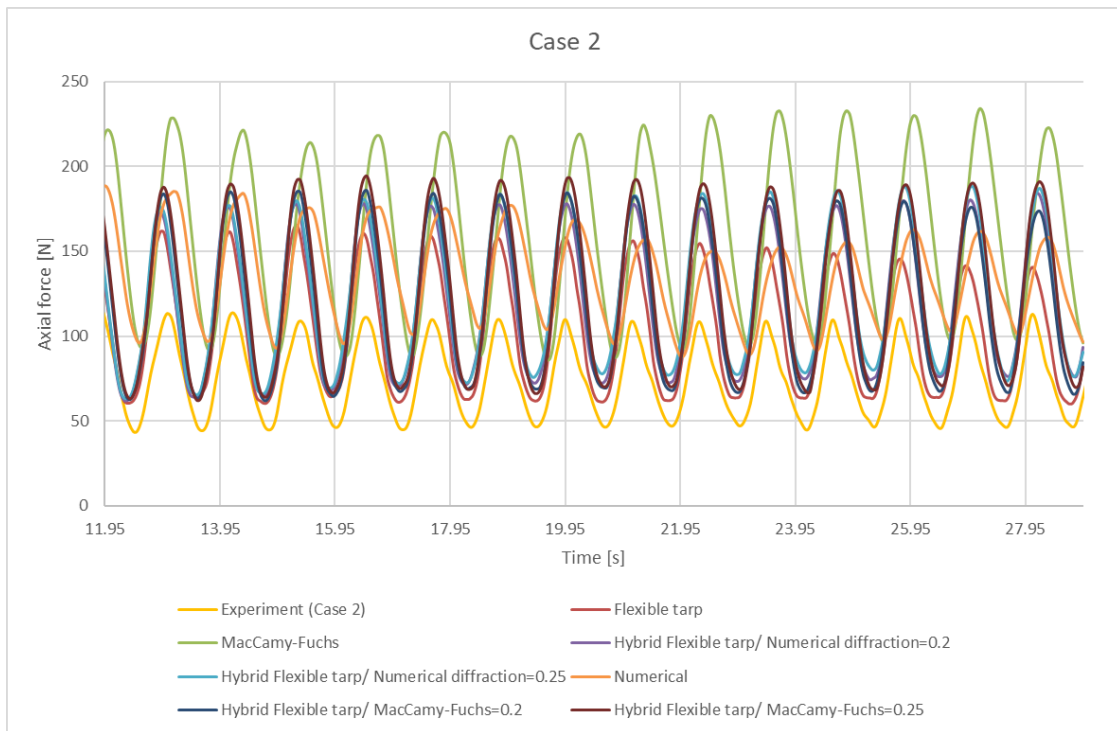


Figure 40 Results Case 2

From Figure 40 it is seen that AquaSim results with diffraction models MacCamy-Fuchs and Numerical predicts a force amplitude that compares very with tank test data “Experiment (Case 2). The other diffraction models predict a force amplitude that is slightly higher than found from tank test. As with Case 1, AquaSim forces are generally at a higher level and hence considered to be on the conservative side.

### Case 3

Average line tension force in the load cell from the tank test is presented in Figure 41.

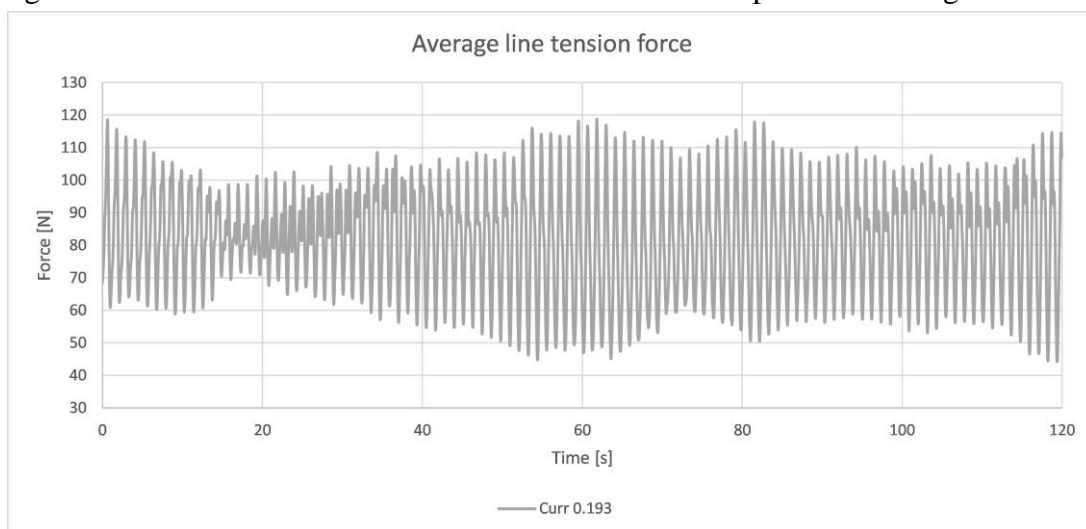


Figure 41 Average line tension force in load cell from tank test

Comparison of experiment (tank test) and AquaSim analysis is presented in Figure 40. “Experiment (Case 3)” are data from the tank test. The other curves are AquaSim analysis results; axial force from the load-cell point, as described in Figure 26.

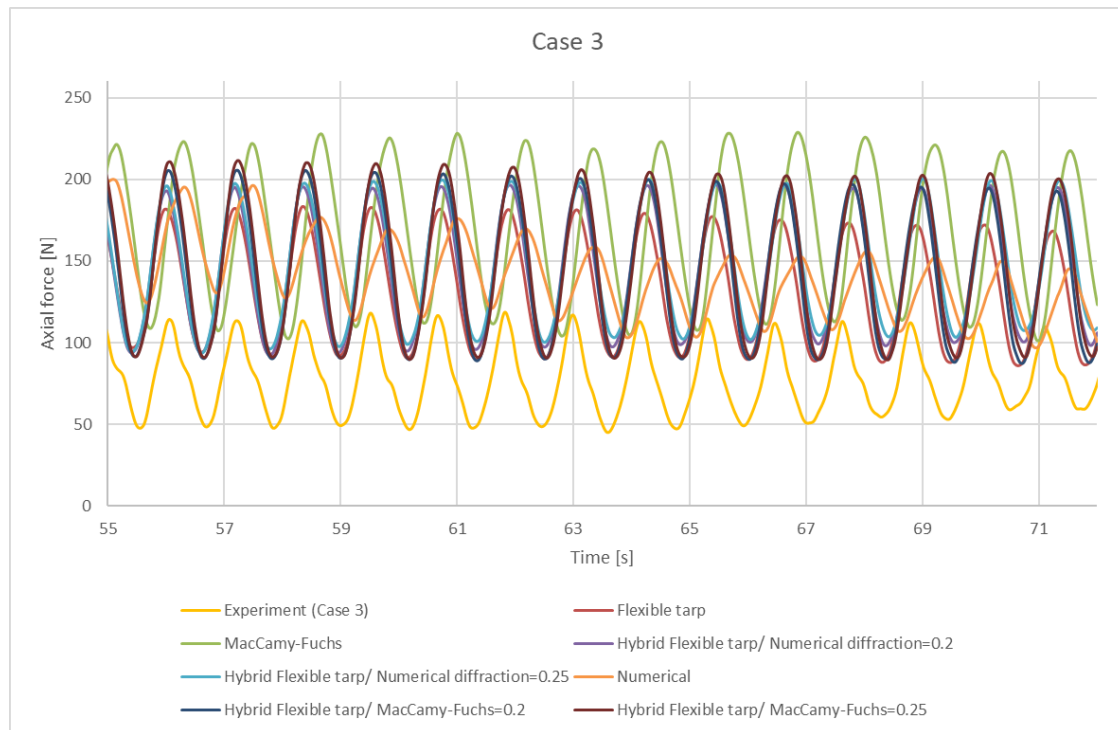


Figure 42 Results Case 3

From Figure 42 it is seen that the AquaSim results, when it comes to the general level and the force amplitude, are higher than found from tank test.

As seen by comparing analysis and measurements, the results compare well for this case with respect to maximum values, but less well for minimum values and the average.


In real life both drag and lift coefficients as well as other properties such as added mass depends strongly on the condition. This means one cannot assume to choose these values and have good fits for all components.

There are also variations in loading in a tank test and there are uncertainties with respect to modelled parameters. This means one cannot assume a better fit than this. To investigate the influence of individual parameters sensitivity studies should be conducted.

### 3.3.3 Results discussion

Results show that there is correspondence between the tank test and AquaSim, especially when applying the diffraction models Flexible tarp and Hybrid Flexible tarp/ Numerical diffraction = 0.2 and 0.25.

As a conclusion, the parameters presented in Table 5 can be applied as base parameters knowing this will provide realistic and numerical stable results in AquaSim.

TR-FOU-2328-5			 Page 40 of 42
Author: HNM	Verified: AJB	Revision: 9	Published: 08.10.2024

## 4 Conclusion


In AquaSim one may choose from several diffraction theories applicable for calculation on loads to stiff bodies.

Case study 1, 2 and 3 shows the applicability of these theories.

Parameters from AquaSim are presented and the effect of loading is shown in graphs in section 3.3.2. What parameters to use for design should be chosen combined with how much other knowledge there is about the system such that conservatism is secured.


Applicable added mass is a complex issue and sensitivity studies should be considered in case of resonance or susceptibility to impact load response.



TR-FOU-2328-5			 Page 41 of 42
Author: HNM	Verified: AJB	Revision: 9	Published: 08.10.2024

## 5 References

- Airy Wave Theory. (2024, 01 28). *Wikimedia Foundation Inc.* Retrieved from Wikipedia: [https://en.wikipedia.org/wiki/Airy\\_wave\\_theory](https://en.wikipedia.org/wiki/Airy_wave_theory)
- Aquastructures. (2013). *On the Analysis of Moored large Mass Floating Objects and how to carry out such Analysis with AquaSim*. Tech. rep. 2174-1. Revision 2.
- Aquastructures. (2016). *Impermeable nets in AquaSim*. Tech. rep. TR-FOU-2692-2.
- Aquastructures. (2019). *Loads on Impermeable Nets and Large Volume Objects in AquaSim*. TR-FOU-2328-5 Revision no. 5.
- Archimede's principle. (2024, 01 26). *Wikimedia Foundation Inc.* Retrieved from Wikipedia: [https://en.wikipedia.org/wiki/Archimedes%27\\_principle](https://en.wikipedia.org/wiki/Archimedes%27_principle)
- Babarit, A., & Delhommeau, G. (2015). Theoretical and numerical aspects of the open source BEM solver NEMOH. *In Proc. of the 11th European Wave and Tidal Energy Conference (EWTEC2015), Nantes France.*
- Barkley, D. (2006). Linear analysis of the cylinder wake mean flow. *Europhys. Lett.* 75 (5), pp. 750-756 DOI: 10.1209/epl/i2006-10168-7.
- Berstad, A., & Heimstad, L. (MARINE 2015, Rome, Italy). Numerical Formulation of Sea Loads to Impermeable nets. *VI International Conference on Computational Methods in Marine Engineering.*
- Egersund Net. (2020). *AquaSim vs modellforsøk - 90x20 m tube i strøm og bølger*. Author: Ketil Roaldsnes.
- Faltinsen, O. (1990). *Sea Loads on Ships and Offshore Structures*. Cambridge University Press. ISBN 0-521-37285-2.
- Flow around a cylinder. (2024, 01 26). *Areodynamics for students*. Retrieved from Figure 4.31A: [http://www-mdp.eng.cam.ac.uk/web/library/enginfo/aerothermal\\_dvd\\_only/aero/fprops/poten/nod\\_e37.html](http://www-mdp.eng.cam.ac.uk/web/library/enginfo/aerothermal_dvd_only/aero/fprops/poten/nod_e37.html)
- Hydrostatics. (2024, 01 26). *Wikimedia Foundation Inc.* Retrieved from Wikipedia: <https://en.wikipedia.org/wiki/Hydrostatics>
- MacCamy, R., & Fuchs, R. (1954). Wave forces on piles: a diffraction theory. *Tech. Memo No. 69. US Army Corps of Engineers.*
- Morison equation. (2024, 01 28). *Wikimedia Foundation Inc.* Retrieved from Wikipedia: [https://en.wikipedia.org/wiki/Morison\\_equation](https://en.wikipedia.org/wiki/Morison_equation)
- Ogawa S., K. Y. (2018). Performance Improvement by Control of Wingtip Vortices for Vertical Axis Type Wind Turbine. *Open Journal of Fluid Dynamics*, pp. 331-342. doi: 10.4236/ojfd.2018.83021.

TR-FOU-2328-5			 Page 42 of 42
Author: HNM	Verified: AJB	Revision: 9	Published: 08.10.2024

SINTEF. (2020). *The North Sea Centre Flume Tank. SINTEF fisheries and Aquaculture, The North Sea Centre. P.O. Box 104 DK-9850 Hirtshals Denmark.*

Wikipedia. (2024d, 05 16). *Stokes drift*. Retrieved from Wikipedia:  
[https://en.wikipedia.org/wiki/Stokes\\_drift](https://en.wikipedia.org/wiki/Stokes_drift)